# FLOW OF A VISCOUS LIQUID ON A ROTATING DISK

Thesis for the Degree of Ph. D.
MICHIGAN STATE UNIVERSITY
Tony Leonard Kaminski
1965





## This is to certify that the

#### thesis entitled

Flow of a Viscous Liquid on a Rotating Disk

presented by

Tony L. Kaminski

has been accepted towards fulfillment of the requirements for

Ph.D. degree in Agricultural Engineering

Major professor

Date 4-29-65

200 A324

		į

#### ABSTRACT

# FLOW OF A VISCOUS LIQUID ON A ROTATING DISK

## by Tony Leonard Kaminski

There are inherent advantages to the rotating disk for the atomization or distribution of liquids especially liquids which cannot be subjected to high pressure or which contain solid particles. An investigation was conducted to obtain a more thorough understanding of the flow of a liquid on a flat rotating disk and to determine the feasibility of using theoretical considerations to study this flow situation. In this study an exact solution to the Navier-Stokes equations, for the case of flow around a disk rotating in a fluid at rest, was applied to the present flow situation. The flow of the liquid on the disk was characterized by means of streamline projections in both the horizontal (r-0) plane and the vertical (r-z) plane.

An experimental apparatus consisting of a 6-inch diameter disk powered by a variable speed motor was used to verify the theoretical results. Two mineral oils were selected for the tests: one had a kinematic viscosity of .087 in<sup>2</sup>/sec and the other had a kinematic viscosity of .194 in<sup>2</sup>/sec. The oil was introduced axially symmetrical

onto the disk through a plexi-glass tube designed to reduce the axial velocity of the liquid. Effects of rotational speeds of 1000 rpm and 2400 rpm and flow rates of 5.0 gpm and 10.2 gpm of the two oils were considered.

The thickness of the oil layer on the disk was measured with a point gage and the streamline patterns in the horizontal plane were photographed. The theoretical and experimental curves were compared and the deviations between some of the curves were explained.

The following conclusions derived from the Navier-Stokes equations were verified experimentally for the laminar flow of a Newtonian fluid on a rotating disk.

- 1. The thickness of the liquid flowing on the disk is increased by: (a) increased liquid viscosity (b) increased flow rate and (c) slower rotational speed.
- 2. The angular displacement of the liquid from inlet to outlet is increased by: (a) increased liquid viscosity
  (b) decreased flow rate and (c) higher rotational speed.
- 3. The angle relative to the radius with which a liquid particle leaves the disk increases with (a) increased angular displacement (b) increased radial distance and (c) decreased height above the disk surface. This angle has a maximum value of 90 degrees on the surface of the disk implying that a particle at this height has only tangential velocity. As the distance above the disk increases the flow becomes more in a radial direction.

Preliminary experiments were made injecting fluid through special nozzles on a section of the disk. These tests showed that approximately two-thirds of the liquid could be made to flow off of one-fifth of the circumference of the disk.

Approved\_

Major Professor

Approved

Department Chairman

# FLOW OF A VISCOUS LIQUID ON A ROTATING DISK

Ву

Tony Leonard Kaminski

#### A THESIS

Submitted to
Michigan State University
in partial fulfillment of the requirements
for the degree of

DOCTOR OF PHILOSOPHY

Department of Agricultural Engineering



#### ACKNOWLEDGMENTS

The author sincerely appreciates the assistance of all who have helped in this study. He is extremely appreciative for the council and guidance provided by Dr. Sverker Persson (Agricultural Engineering) during his research work.

To the other members of the guidance committee,

Professor H. F. McColly (Agricultural Engineering),

Dr. N. L. Hills (Mathematics) and Dr. G. E. Mase (Metallurgy,

Mechanics, and Material Science) the author expresses his

gratitude for their time, professional interests, and con
structive criticisms.

Dr. M. Krzywoblocki (Mechanical Engineering) made many helpful suggestions during the theoretical considerations in this study. Professor C. M. Hansen (Agricultural Engineering) was instrumental in obtaining the financial grant, from the American Oil Company, Whiting, Indiana, for the assistantship which made this work possible. Mr. James Cawood and his staff in the Agricultural Engineering Research Laboratory assisted in the development of the experimental apparatus.

This dissertation is dedicated to my wife, Zena, who consistently gave her encouragement and support to this study.

		,
		,
		?

# TABLE OF CONTENTS

														Page
ACKNOWLE	DGMENT	rs .		•		•	•		•	•			•	ii
LIST OF	TABLES	· .	•	•		•	•	•	•	•	•	•	•	iv
LIST OF	FIGURE	ES .	•	•		•		•	•	•	•		•	v
LIST OF	APPEND	DICES	TAE	BLES						•		•	•	viii
ABBREVIA	TIONS	AND S	SYME	BOLS						•		•	•	х
Chapter														
I.	INTRO	DUCT	ION				•			•		•	•	1
II.	REVIE	W OF	LIT	ERAT	CURE		•			•		•	•	6
III.	THEOF	RETICA	AL C	CONSI	DER	ATI	ONS			•		•	•	11
	_	The Fine Desci	luid	and	i an	In	fini	te I	Disk			•	•	11 19
IV.	EXPER	RIMENT	ΓAL	CONS	SIDE	RAT	IONS	•		•		•	•	27
	4.2		ctic	on of	: a	Vis	cous	Lic	quid	l.	•	•	•	27 32 33
٧.	PRESE	CTATI	ION	AND	DIS	CUS	SION	OF	RES	ULT	'S	•	•	38
	5.1 5.2 5.3	Strea	amli	nes	in	the	r−0	Pla	ane	•		• •	•	38 52
	ر. 5		lsk			<b>.</b>	•	•	•	•	•	•	•	62
VI.	SUMMA	ARY Al	1D C	CONCI	LUSI	ONS	•			•		•	•	71
	6.1 6.2	Summa Concl	ary lusi	.ons	•	•				•	•	•		71 73
SUGGESTI	ONS FO	R FUE	RTHE	ER ST	rudy	•		•	•	•		•	•	76
REFERENC	ES	•	•			•		•	•	•			•	77
V P P E N D T C	FC													80

# LIST OF TABLES

Page		Table
18	Functions for the velocity and pressure distribution as calculated by the digital computer using equations 3.29 - 3.34	1.
36	Values of specific gravity and kinematic viscosity obtained from samples of the oils used in the laboratory tests	2.
38	Tests conducted to study the flow of a viscous liquid on a rotating disk	3.
44	Comparison of experimental and theoretical axial velocities at the tube outlet, located .300 inches above the surface of the disk, with the experimental resultant velocity at the edge of the disk	4.
47	Values of Reynolds numbers present in the laboratory tests	5.
63	Comparison of the experimental and theoretical surface streamlines using angular displacements and angles relative to the radius at the edge of the disk	6.
64	Comparison of the experimental and theoretical average radial and average tangential velocities at the edge of the disk	7.

# LIST OF FIGURES

Figure		Pa	age
1.	Flow near a disk rotating in a fluid at rest.  Velocity components: u-radial, v-circum- ferential and w-axial	•	12
2.	Example of radial and tangential velocity profiles above a rotating disk	•	21
3.	Motion of a particle on a rotating disk	•	24
4.	Example of how the ratio of tangential velocity to radial velocity varies with radial position on the disk	у •	25
5.	The testing apparatus (MSU Photo No. 65772-10)	•	28
6.	The point gage and plexi-glass tube mounted above the disk (MSU photo No. 65772-11) .	•	29
7.	Equipment used for flow measurement (MSU Photo No. 65772-12)	•	31
8.	Comparison of experimental and theoretical streamlines in the r-z plane for hydraulic oil ( $\nu$ = .194 in²/sec) flowing on a disk rotating at 1000 rpm	•	39
9.	Comparison of experimental and theoretical streamlines in the r-z plane for hydraulic oil ( $\nu$ = .194 in²/sec) flowing on a disk rotating at 2400 rpm	•	40
10.	Comparison of experimental and theoretical streamlines in the r-z plane for mineral oil ( $\nu$ = .087 in²/sec) flowing on a disk rotating at 1000 rpm	•	41
11.	Comparison of experimental and theoretical streamlines in the r-z plane for mineral oil ( $\nu$ = .087 in <sup>2</sup> /sec) flowing on a disk rotating at 2400 rpm	•	42

12.	Comparison of experimental and theoretical radial velocity profiles on a disk rotating at 2100 rpm in air (obtained by Gregory et al. 1955) Curve 1, theoretical laminar profile; 2, 3, 4 experimental profiles: 2, laminar region; 3, instability region; 4, turbulent region	49
13.	Comparison of experimental and theoretical tangential velocity profiles on a disk rotating at 2100 rpm in air (obtained by Gregory et al. 1955) Curve 1, theoretical laminar profile; 2, 3, 4 experimental profiles: 2, laminar region; 3 instability region; 4, turbulent region	50
14.	Comparison of experimental and theoretical streamlines in the r-0 plane for 10.2 gpn flow of hydraulic oil ( $\nu$ = .194 in²/sec) onto a disk rotating at 1000 rpm (clockwise) (MSU Photo No. 65772-2)	53
15.	Comparison of experimental and theoretical streamlines in the r-0 plane for 10.2 gpm flow of hydraulic oil ( $\nu$ = .194 in²/sec) onto a disk rotating at 2400 rpm (clockwise) (MSU Photo No. 65772-3)	54
16.	Comparison of experimental and theoretical streamlines in the r-0 plane for 5.0 gpm flow of hydraulic oil (v = .194 in²/sec) onto a disk rotating at 1000 rpm (clockwise) (MSU Photo No. 65772-4)	55
17.	Comparison of experimental and theoretical streamlines in the r-0 plane for 5.0 gpm flow of hydraulic oil (v = .194 in²/sec) onto a disk rotating at 2400 rpm (clockwise) (MSU Photo No. 65772-1)	56
18.	Comparison of experimental and theoretical streamlines in the r-0 plane for 10.2 gpm flow of mineral oil (v = .087 in²/sec) onto a disk rotating at 1000 rpm (clockwise) (MSU Photo No. 65772-5)	57

igure		Page
19.	Comparison of experimental and theoretical streamlines in the r-0 plane for 10.2 flow of mineral oil ( $\nu$ = .087 in²/sec) onto a disk rotating at 2400 rpm (clockwise) (MSU Photo No. 65772-6)	) . 58
20.	Comparison of experimental and theoretical streamlines in the r-0 plane for 5.0 gpm flow of mineral oil ( $\nu$ = .087 in²/sec) onto a disk rotating at 1000 rpm (clockwise) (MSU Photo No. 65772-7)	) • 59
21.	Comparison of experimental and theoretical streamlines in the r-0 plane for 5.0 gpm flow of mineral oil ( $\nu$ = .087 in²/sec) onto a disk rotating at 2400 rpm (clockwise) (MSU Photo No. 65772-8)	) . 60
22.	Closed-bottom nozzle (left) and open-bottom nozzle (right) with parrallelogram-shaped openings (MSU Photo No. 65772-9)	. 66
23.	Diagram of a parallelogram-shaped nozzle opening (MSU Photo No. 65772-9)	. 66
24.	Flow pattern from the closed-bottom nozzle (N = 1000 rpm, Q = 4.4 gpm, \(\nu = .194 in/\)sec (MSU Photo No. 65772-13)	) . 69
25.	Streamlines in the r-0 plane for the closed-bottom nozzle (N = 1000 rpm, Q = 4.4 gpm, $\nu$ = .194 in <sup>2</sup> /sec) (MSU Photo No. 65772-14)	. 69
26.	Flow pattern from the open-bottom nozzle (N = 1000 rpm, Q = 5.4 gpm, $v$ = .194 in 2/sec) (MSU Photo No. 65772-15)	) . 70
27.	Streamlines in the r-0 plane for the open- bottom nozzle (N = 1000 rpm, Q = 5.4 gpm, $\nu$ = .194 in <sup>2</sup> sec) (MSU Photo No. 65772-16)	. 70
	Negatives of photographs are filed by Information Services, Michigan State University	ion

F

## LIST OF APPENDICES TABLES

Appendix A		Page
Al.	Dimensionless radial (F) and tangential (G) velocity components for hydraulic oil (v = .194 in²/sec.) flowing on a disk rotating at both 1000 rpm and 2400 rpm	81
A2.	Radial velocity components for hydraulic oil ( $v = .194 \text{ in}^2/\text{sec.}$ ) flowing on a disk rotating at 1000 rpm	82
А3.	Tangential velocity components for hydraulic oil ( $\nu$ = .194 in 2/sec.) flowing on a disk rotating at 1000 rpm	83
А4.	Radial velocity components for hydraulic oil ( $v = .194 \text{ in}^2/\text{sec.}$ ) flowing on a disk rotating at 2400 rpm	84
A5.	Tangential velocity components for hydraulic oil ( $\nu$ = .194 in <sup>2</sup> /sec.) flowing on a disk rotating at 2400 rpm	85
A6.	Dimensionless radial (F) and tangential (G) velocity components for mineral oil ( $\nu$ = .087 in²/sec.) flowing on a disk rotating at both 1000 rpm and 2400 rpm.	86
A7.	Radial velocity components for mineral oil ( $\nu = .087 \text{ in}^2/\text{sec.}$ ) flowing on a disk rotating at 1000 rpm	87
A8.	Tangential velocity components for mineral oil ( $v = .087 \text{ in}^2/\text{sec.}$ ) flowing on a disk rotating at 1000 rpm	88
A9.	Radial velocity components for mineral oil ( $\nu = .087 \text{ in}^2/\text{sec.}$ ) flowing on a disk rotating at 2400 rpm	89
AlO.	Tangential velocity components for mineral oil ( $v = .087 \text{ in}^2/\text{sec.}$ ) flowing on a disk rotating at 2400 rpm.	90

Appendix B		Page
B1.	Determination of streamlines in r-0 plane for 10.2 gpm flow of hydraulic oil (v = .194) onto a disk rotating at 1000 rpm	92
В2.	Determination of streamlines in $r-\theta$ plane for 10.2 gpm flow of hydraulic oil ( $\nu$ = .194) onto a disk rotating at 2400 rpm	93
В3.	Determination of streamlines in $r-\theta$ plane for 5.0 gpm flow of hydraulic oil ( $\nu$ = .194) onto a disk rotating at 1000 rpm	94
В4.	Determination of streamlines in r-0 plane for 5.0 gpm flow of hydraulic oil (v = .194) onto a disk rotating at 2400 rpm	95
B5.	Determination of streamlines in r-0 plane for 10.2 gpm flow of mineral oil ( $\nu$ = .087) onto a disk rotating at 1000 rpm	96
В6.	Determination of streamlines in r-θ plane for 10.2 gpm flow of mineral oil (ν = .087) onto a disk rotating at 2400 rpm	97
В7.	Determination of streamlines in r-0 plane for 5.0 gpm flow of mineral oil (v = .087) onto a disk rotating at 1000 rpm	98
в8.	Determination of streamlines in r-0 plane for 5.0 gpm flow of mineral oil (v = .087) onto a disk rotating at 2400 rpm	99

# ABBREVIATIONS AND SYMBOLS

А	area
cm	Centimeter
eq	equation
F	dimensionless radial velocity
G	dimensionless tangential velocity
Н	dimensionless axial velocity
in	inch
in <sup>2</sup>	square inch
ips	inches per second
1b	pound
ln	logarithm to the natural base, e
N	rotational speed
No.	number
p	pressure
P	nondimensional pressure
Q	flow rate
r	radius
Re	Reynolds number
rpm	revolutions per minute
sec	second
t	time
u	radial velocity
v	tangential velocity
W	axial velocity
z	distance normal to disk
θ	angular displacement
ρ	density
μ	absolute viscosity
ν	kinematic viscosity
ω	angular velocity
ζ	dimensionless distance normal to disk

#### I. INTRODUCTION

This study was initiated when working on problems in connection with the atomization of a liquid emulsion which could not be atomized by more conventional methods.

Hougthon (1950) and Bainer et al. (1955) stated that in general, devices used for the atomization of liquids utilize one or more of the following principles:

- 1. Pressure or hydraulic atomization, in which liquid pressure supplies the atomization energy. The liquid stream from the nozzle or an orifice is broken up by its inherent instability and its inpact upon the atmosphere or by impact upon a plate or another jet. In some designs liquid pressure is used for obtaining rotary motion within the nozzle.
- 2. Gas atomization, in which the liquid is broken up by a high velocity gas stream, the breakup occuring either entirely outside of the nozzle or within a chamber ahead of the exit orifice.
- 3. Centrifugal atomization, in which the liquid is fed under low pressure to the center of a rotating device, such as a disk or cup, and is broken up by centrifugal force as it leaves the periphery.

The hydraulic-type spray nozzle is the most common atomizing device. It in general can be successfully used to atomize most of the common liquids. This device does however possess certain limitations which have compelled the use of other devices. High viscosities may necessitate heating the liquid before it can be forced through the nozzle to be atomized. Since atomization is influenced by the size of the nozzle orifice, high pressures are required in order to maintain both reach and atomization.

Unstable liquid emulsions and various liquid mixtures such as liquid manure cannot be dispersed by spray nozzles and they have necessitated atomization by a rotating disk. The problem presented by the unstable emulsion is that the pressure required to force the liquid through the nozzle may cause the liquid to harden in the pump or at the nozzle. Whereas the problem encountered with a non-homogeneous liquid such as liquid manure is that of clogging of the nozzle which cannot be satifactorily corrected by the use of filters.

Although the principle of centrifugal atomization is not common in liquid sprayers, Yates (1951) and Gunkel (1957) have shown that it is a very successful method of producing uniform droplet sizes. In addition there are inherent virtues to the design of a centrifugal device:

- 1. Simplicity
- 2. Low cost
- 3. Compact dimensions for a given width of coverage
- 4. No close tolerances or small holes required
- 5. Material is fed by gravity or a low pressure pump

Due to these advantages the rotating disk is used extensively today for the distribution of granular materials. Patterson and Reece (1962) analyzed the motion of spherical particles fed on to the center of a rotating disk fitted with radial vanes. They checked their theoretical results by feeding steel balls on to the center of the disk. Inns and Reece (1962) extended the theory to the case of off-center feeding of spherical particles on to a plate fitted with radial vanes. The effect of impact between the particle and vane was taken into account. Experimental evaluation of the theory showed that the path of a spherical particle accelerated by a flat radial vane may be accurately calculated.

Crowther (1958) investigated how factors such as disk speed, fertilizer particle size, forward travel of the disk and overlapping of adjacent runs affect the pattern of spread of granular fertilizer distributed by a centrally-fed spinning disk fitted with radial vanes.

These studies have yielded some information for the design of a disk for the distribution of granular particles. Little, however, is known about the design of a disk for the handling of a viscous liquid. Various theoretical

considerations have been made on the flow of fluids due to the presence of a rotating disk but it appears as if none of the theory has been applied to the flow of liquids and no experimental evaluations have been made.

The designs of some of the existing centrifugal atomizing devices have followed a trial and error procedure. It is well known that when the liquid is introduced axially symmetrical on to a flat rotating disk, the liquid is uniformly atomized about the entire periphery of the disk. For this reason the rotating disk may not be suitable for certain applications requiring a fan-like spray pattern similar to the pattern produced by a spray nozzle. It is suggested that if sufficient information was available on the movement of liquid on a rotating disk then it may be possible to produce any desired form of spray pattern with a disk by precise introduction of the liquid on to a specific area of the disk.

The purpose of this research work was to:

- 1. Fully develop the theory of axial-symmetric flow of a viscous liquid on to a flat rotating disk and characterize the flow by constructing various flow profiles and streamline representations.
- 2. Experimentally evaluate the theory using a laboratory apparatus.

- 3. Study the effect of viscosity, flow rate and rotational speed of the disk on the flow of the liquid.
- 4. Present a hypothesis for producing a specific form of spray pattern and verify it experimentally.

#### II. REVIEW OF LITERATURE

The steady flow of a viscous fluid, due to an infinite rotating disk, was first discussed by von Karman (1921). He studied the case where the fluid occupied the semi-infinite region on one side of the disk and the motion of the fluid could be assumed to be rotationally symmetric around the axis of the disk. The layer of fluid near the disk was put in rotary motion by the disk through viscous friction and thrown outwards owing to the action of centrifugal force. This caused a flow of the fluid in the axial direction toward the center of the disk.

By virtue of his assumptions about the velocity components, von Karman could reduce the Navier-Stokes equations to a set of ordinary, non-linear differential equations of a single independent variable. The resulting equations are the boundary-layer equations for this flow situation since the terms which are ordinarily omitted in boundary-layer theory vanish identically. Numerical integration of this set of equations thus yields an exact solution to the Navier-Stokes equations.

Von Karman obtained an approximate solution to the reduced flow equations by using the integral method he developed. Cochran (1934) corrected von Karman's solution

and calculated more accurate values by numerical integration of the ordinary differential equations.

Hömann (1936) considered a related problem of motion of a fluid flowing with axial symmetry towards an infinite stationary plane.

Bödewadt (1940) solved numerically the problem of the flow produced over an infinite stationary plane in a fluid which rotated with uniform angular velocity at an infinite distance from the plane.

Hannah (1947) considered the general question of steady irrotational flow with axial symmetry against an infinite rotating plane. She obtained two solutions: one for a non-viscous liquid and the other for a viscous liquid.

Batchelor (1951) considered two classes or families of solutions of the Navier-Stokes equations representing steady rotationally-symmetric flow. In the first class (one-parameter families) of solutions he showed that a simple form of solution similar to von Kármán's solution is retained if the fluid at infinity had an arbitrary uniform angular velocity about the axis of rotation of the infinite disk. In the second class (two-parameter families) of solutions Batchelor described the flow between two parallel infinite disks rotating about the same axis with different angular velocities.

Von Schlichting and Truckenbrodt (1952) considered laminar flow of the fluid around a finite rotating disk

moving through an infinite fluid at a uniform axially velocity and concluded that the thickness of the layer carried along by the rotating disk depended mainly on the ratio of the axial velocity of the disk and the peripheral velocity of the disk. Truckenbrodt (1954) studied turbulent boundary layer at the surface of the rotating disk and concluded that the thickness of the boundary layer and also the torque of the rotating disk depended strongly on the ratio of the axial velocity of the disk to the peripheral velocity of the disk.

Stewartson (1953) considered theoretically and experimentally the steady motion of a viscous fluid confined between two coaxial rotating disks. He found experimentally that when the disks rotate in the same direction the main body of the fluid rotated as well, but if the disks rotate in opposite directions the main body of the fluid was almost at rest.

Stuart (1954) integrated the exact ordinary differential equations of von Kármán for the case of fluid being sucked through the disk. In the analysis a suction parameter a was introduced, where a vww was the velocity of suction acting normal to the disk. He found that the magnitude of the radial flow velocity decreased rapidly as the suction increased, while at the disk the derivative of the tangential component with respect to the distance from the disk increased.

In 1955 Fettis devised an iterative process for obtaining approximate solutions for several cases of rotationally symmetric flow in which the fluid at infinity was rotating at an arbitrary velocity in the same direction as the disk. Leigh (1955) developed a method for use with an electronic computer for solving the laminar boundary—layer equation. Wu (1961) discussed the finite difference solution to laminar boundary—layer problems.

Rogers and Lance (1960) investigated numerically the flow produced by an infinite rotating disk when the fluid at infinity was in the state of solid rotation. the fluid at infinity was rotating in the same direction as the disk, physically acceptable solutions were present in all cases. When the fluid at infinity rotated in the Opposite direction to the disk the only acceptable solutions Were where there was uniform suction present acting through the disk. Rogers and Lance (1962) also considered axially symmetric flow of a viscous fluid between two infinite rotating disks. Several cases were investigated in detail and the radial and transverse velocity profiles were presented. When one disk was at rest or both disks were rotated in the same direction, the flow at high Reynolds numbers could be represented by combining two one-disk solutions. There were boundary layers attached to both disks and in the main body of the fluid, the flow was from the slower to the faster disk.

Von Kármán and Lin (1961) proved the existence of an exact solution of the Navier-Stokes equations. The literature review may be summarized by stating that in 1921 von Kármán showed that the flow due to an infinite rotating disk could be treated by an exact solution of the Navier-Stokes equations, provided that a certain boundary-value problem involving a system of nonlinear ordinary differential equations could be solved. Various mathematical solutions related to this flow situation were presented within this forty-year period, but it wasn't until 1961 that a mathematical proof was provided to the fact that this boundary value problem did possess a solution. This literature review had indicated that no attempts have been made to study non-symmetrical motion of the fluid due to a rotating disk nor have any studies been made on the flow of a finite quantity of liquid with a limited thickness and a free upper surface.

#### III. THEORETICAL CONSIDERATIONS

# 3.1 The Flow Functions for a Semi-Infinite Fluid and an Infinite Disk

The Navier-Stokes equations express the condition of equilibrium between the forces due to pressure, viscosity, inertia and gravity for a fluid in motion. In 1921 von Kármán applied the Navier-Stokes equations to the flow near an infinite flat disk which rotated with an angular Velocity  $\omega$  in a semi-infinite fluid at rest. A layer of fluid is propelled around by the disk through viscous friction and is at the same time thrown outwards due to centrifugal force. This causes a flow in an axial direction towards the disk to replace the fluid thrown out. This is a three-dimensional flow case, i.e. there exist velocity components in the radial direction, r, the circumferential direction,  $\theta$ , and the axial direction, z, which will be denoted respectively by u, v, and w. An axonometric representation of this flow is shown in Figure 1. The general system of Navier-Stokes equations in cylindrical co-ordinates for the case of incompressible fluid flow (Schlichting, 1960) are:

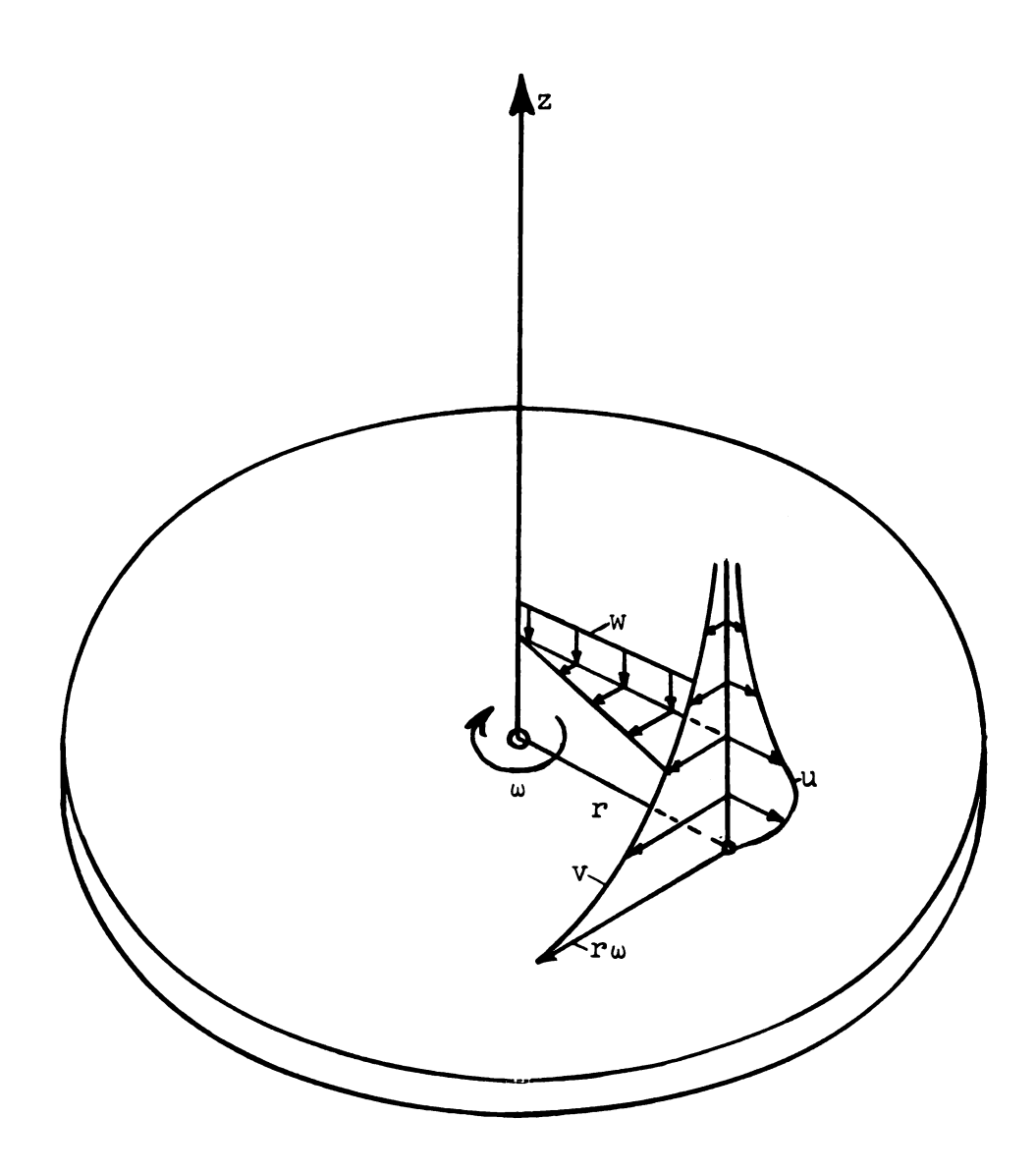


Figure 1. Flow near a disk rotating in a fluid at rest. Velocity components: u-radial, v-circumferential and w-axial.

$$\rho \left( \frac{\partial u}{\partial t} + u \frac{\partial u}{\partial r} + v \frac{\partial u}{\partial \theta} - \frac{v^2}{r} + w \frac{\partial u}{\partial z} \right) = F_r - \frac{\partial p}{\partial r} + \mu \left( \frac{\partial^2 u}{\partial r^2} + \frac{1}{r} \frac{\partial u}{\partial r} \right)$$

$$- \frac{u}{r^2} + \frac{1}{r^2} \frac{\partial^2 u}{\partial \theta^2} - \frac{2}{r^2} \frac{\partial v}{\partial \theta} + \frac{\partial^2 u}{\partial z^2} \right)$$

$$(3.1)$$

$$\rho \left( \frac{\partial \mathbf{v}}{\partial \mathbf{t}} + \mathbf{u} \frac{\partial \mathbf{v}}{\partial \mathbf{r}} + \frac{\mathbf{v}}{\mathbf{r}} \frac{\partial \mathbf{v}}{\partial \theta} + \frac{\mathbf{u} \mathbf{v}}{\mathbf{r}} + \mathbf{w} \frac{\partial \mathbf{v}}{\partial z} \right) = \mathbf{F}_{\theta} - \frac{1}{\mathbf{r}} \frac{\partial \mathbf{p}}{\partial \theta} + \mu \left( \frac{\partial^{2} \mathbf{v}}{\partial \mathbf{r}^{2}} \right)$$

$$+ \frac{1}{\mathbf{r}} \frac{\partial \mathbf{v}}{\partial \mathbf{r}} - \frac{\mathbf{v}}{\mathbf{r}^{2}} + \frac{1}{\mathbf{r}^{2}} \frac{\partial^{2} \mathbf{v}}{\partial \theta^{2}} + \frac{2}{\mathbf{r}^{2}} \frac{\partial \mathbf{u}}{\partial \theta} + \frac{\partial^{2} \mathbf{v}}{\partial z^{2}}$$

$$(3.2)$$

$$\rho \left( \frac{\partial w}{\partial t} + u \frac{\partial w}{\partial r} + \frac{v}{r} \frac{\partial w}{\partial \theta} + w \frac{\partial w}{\partial z} \right) = F_z - \frac{\partial p}{\partial z} + \mu \left( \frac{\partial^2 w}{\partial r^2} + \frac{1}{r} \frac{\partial w}{\partial r} + \frac{1}{r} \frac{\partial w}{\partial z} \right)$$

$$+ \frac{1}{r^2} \frac{\partial^2 w}{\partial \theta^2} + \frac{\partial^2 w}{\partial z^2}$$

$$(3.3)$$

Continuity equation:

$$\frac{\partial u}{\partial r} + \frac{u}{r} + \frac{1}{r} \frac{\partial v}{\partial \theta} + \frac{\partial w}{\partial z} = 0 \tag{3.4}$$

Where

 $\rho$  = mass density

t = time

p = pressure

F = body force

 $\mu$  = absolute viscosity

u, v, w = velocity components

By neglecting the body forces and assuming steady rotationally symmetric flow of a viscous liquid the Navier-Stokes equations can be written as  $u \frac{\partial u}{\partial r} - \frac{v}{r}^2 + w \frac{\partial u}{\partial z}$ 

$$= -\frac{1}{\rho} \frac{\partial p}{\partial r} + \nu \left( \frac{\partial^2 u}{\partial r^2} + \frac{1}{r} \frac{\partial u}{\partial r} - \frac{u}{r^2} + \frac{\partial^2 u}{\partial z^2} \right)$$
 (3.5)

$$u \frac{\partial v}{\partial r} + \frac{uv}{r} + w \frac{\partial v}{\partial z} = v \left( \frac{\partial^2 v}{\partial r^2} + \frac{1}{r} \frac{\partial v}{\partial r} - \frac{v}{r^2} + \frac{\partial^2 v}{\partial z^2} \right)$$
(3.6)

$$u \frac{\partial w}{\partial r} + w \frac{\partial w}{\partial z} = -\frac{1}{\rho} \frac{\partial p}{\partial z} + v \left( \frac{\partial^2 w}{\partial r^2} + \frac{1}{r} \frac{\partial w}{\partial r} + \frac{\partial^2 w}{\partial z^2} \right)$$
(3.7)

$$\frac{\partial \mathbf{u}}{\partial \mathbf{r}} + \frac{\mathbf{u}}{\mathbf{r}} + \frac{\partial \mathbf{w}}{\partial z} = 0 \tag{3.8}$$

Where  $v = \frac{\mu}{\rho} = \text{kinematic viscosity}$ 

The no-slip condition on the disk gives the following boundary conditions

$$z = 0 : u = 0, v = rw w = 0$$
 (3.9)

and the condition of a fluid at rest at infinity gives

$$z = \infty : u = 0, v = 0 \dots$$
 (3.10)

The equations of motion and the continuity equation are satisfied by the following substitutions:

$$u = rf(z), v = rg(z), w = h(z), p = p(z)...(3.11)$$

These assumptions can be used only in laminar flow since in turbulent flow the velocity components are not proportional to the radius but more complicated functions of the radius. Assuming laminar flow, the Navier-Stokes equations become

$$f^2 - g^2 + h \frac{df}{dz} - v \frac{d^2 f}{dz^2} = 0$$
 (3.12)

$$2fg + h \frac{dg}{dz} - v \frac{d^2g}{dz^2} = 0$$
 (3.13)

$$h\frac{dh}{dz} + \frac{1}{\rho} \frac{dp}{dz} - v\frac{d^2h}{dz^2} = 0$$
 (3.14)

$$2\mathbf{f} + \frac{d\mathbf{h}}{dz} = 0 \tag{3.15}$$

with the following boundary conditions

$$z = 0$$
:  $f = 0$ ,  $g = \omega$ ,  $h = 0$ ,  $p = p_0$  (3.16)

$$z = \infty$$
:  $f = 0$ ,  $g = 0$ ,  $h = -c$ ,  $p = 0$  (3.17)

In order to integrate the system of equations
(3.12-3.15) it is convenient to introduce a dimensionless distance from the disk

$$\zeta = z \sqrt{\frac{\omega}{\nu}} \tag{3.18}$$

The flow equations are also changed into non-dimensional form by substituting

$$f = \omega F(\zeta)$$
,  $g = \omega G(\zeta)$ ,  $h = \sqrt{v\omega} H(\zeta)$ ,  $p = \rho v \omega P_1(\zeta)$ 
(3.19)

where  $P_1 = P - P_0$ 

Thus the following assumptions are made for the velocity components and the pressure:

$$u = \omega r F(\zeta), \quad v = r\omega G(\zeta), \quad w = \sqrt{v\omega} H(\zeta), \quad p = \rho v\omega P_1(\zeta)$$
(3.20)

Inserting these assumptions (3.20) into equations 3.5-3.8 and noting that  $\frac{d}{dz} = \frac{d}{d\zeta} \cdot \frac{d\zeta}{dz}$  yields the following system of four simultaneous, ordinary, non-linear differential equations for the functions F, G, H, and P<sub>1</sub>

$$F^{2} - G^{2} + \frac{dF}{d\zeta} - \frac{d^{2}F}{d\zeta^{2}} = 0$$
 (3.21)

$$2FG + H \frac{dG}{d\zeta} - \frac{d^2G}{d\zeta^2} = 0$$
 (3.22)

$$\frac{\mathrm{d}P_1}{\mathrm{d}\zeta} + H \frac{\mathrm{d}H}{\mathrm{d}\zeta} - \frac{\mathrm{d}^2H}{\mathrm{d}\zeta^2} = 0 \tag{3.23}$$

$$2F + \frac{dH}{d\zeta} = 0 ag{3.24}$$

The boundary conditions calculated from equations (3.9) and (3.10) are:

$$\zeta = 0$$
: F = 0, G = 1, H = 0, P<sub>1</sub> = 0 (3.25)

$$\zeta = \infty : F = 0, G = 0$$
 (3.26)

As indicated earlier the first solution of this system of equations (3.21 - 3.24) was given by von Kármán (1921) by an approximate integral method. Later Cochran (1934) calculated more accurate values, for a limited number of values of the independent variable, by a method of numerical integration. Cochran's solution was obtained by assuming a power series near  $\zeta = 0$  and an asymptotic series for large values of  $\zeta$ . By trial and error he connected the two series which yielded the following boundary conditions for  $\frac{dF}{d\zeta}$  and  $\frac{dG}{d\zeta}$ :

$$\zeta = 0 : \frac{dF}{d\zeta} = 0.510, \frac{dG}{d\zeta} = -0.616$$
 (3.27)

In order to use an existing computer program and solve the equations by a digital computer the dependent variables F, G, H, and  $P_1$  were redefined as follows:

$$y_1 = H$$
,  $y_2 = F$ ,  $y_3 = \frac{dF}{d\zeta}$ ,  $y_4 = G$ ,  $y_5 = \frac{dG}{d\zeta}$ ,  $y_6 = P_1 = P - P_O$  (3.28)

The system of flow equations (3.21 - 3.24) were then written as a system of six first-order linear differential equations for the functions  $y_1$ ,  $y_2$ ,  $y_3$ ,  $y_4$ ,  $y_5$ , and  $y_6$ :

$$\frac{dy_1}{d\zeta} = -2y_2 \tag{3.29}$$

$$\frac{dy_2}{d\xi} = y_3 \tag{3.30}$$

$$\frac{dy_3}{d\zeta} = y_1y_3 + y_2^2 - y_4^2 \tag{3.31}$$

$$\frac{dy_4}{d\zeta} = y_5 \tag{3.32}$$

$$\frac{dy_5}{d\zeta} = 2 y_2 y_4 + y_1 y_5 \tag{3.33}$$

$$\frac{dy_6}{d\zeta} = 2y_1y_2 - 2y_3 \tag{3.34}$$

The original boundary condions (3.24 - 3.25) became  $\zeta = 0$ :  $y_1 = 0$ ,  $y_2 = 0$ ,  $y_3 = 0.510$ ,  $y_4 = 1.0$ ,  $y_5 = -.616$ ,  $y_6 = 0$  (3.35)

The values of the functions of velocity and pressure were calculated by the Michigan State University digital computer (CDC 3600), using library program D2 UTEX RKAMPDP, and are shown in Table 1. The values are shown with four decimal places but the fourth figure is insignificant since some of the initial conditions were accurate to only three significant figures. Many of the very small values shown in Table 1 might be assumed to be zero.

TABLE 1. Functions for the velocity and pressure distribution as calculated by the digital computer using equations 3.29 - 3.34.

$\zeta = z\sqrt{\frac{\omega}{\nu}}$	-Н	F	dF/dζ	G	-dG∕dζ	-P <sub>1</sub>
01234567890123456789012345678902468024680 000000001111111111222222222333333444445	008978889223013426600449083678889931729 0001372888922301342660044908367804889931729 000100001152603373555566678013453899931729 1122603373555556667780133899931729 1122603373555556667780138888888888888888888888888888888888	02633358075955336405052137444855583950540176 00481363548759553364050521377444855583950540176 113547773825811114999488255839505401111111111111111111111111111111111	000688753354293514688519182320866546353646224 1136315329466492851918232086546353646224 110000000000000000000000000000000000	1.093880 0060 00880 00880 009380 009380 00	03884839583434621309262963824390094332055061880724679048631309262973976555555441863332222221116988765433222111110008765433222111111111111111111111111111111111	04335235134352983431975445793713616318754 09627136667703555543209876543322100999999999999999999999999999999999

TABLE 1 (Continued)

$\zeta = z \sqrt{\frac{\omega}{v}}$	–Н	F	dF/dζ	G	-dG/dζ	-P <sub>1</sub>
5.468.02468.0505050.5011.2.   24688.02688.05050505011.2.   24688.02688.0505050505050505050505050505050505050	.8640 .8640 .86690 .87238 .877562 .877652 .87788 .87799 .87999 .87999 .87999 .8786*	.0089 .0074 .0062 .0052 .0043 .0036 .0025 .0020 .0017 .0009 .0007 .0006 .0001 0001 0002 0002	007900670067004700400033002400200017001400080007000400010001000100010000	.0103 .0083 .0086 .0052 .0040 .0030 .0022 .0015 .0009 .0006 0006 0014 0017 0018 0019 0021 0021	.0109 .0091 .0077 .0064 .0054 .0038 .0032 .0022 .0019 .0013 .0011 .0009 .0004 .0004 .0003 .0001 .0000	.3883 .3882 .38881 .38879 .388776 .388776 .388775 .388771 .388679 .388679 .38879 .38979 .38979 .38979 .38979 .38979 .38979 .38979 .38979 .38979 .38979 .38979 .38979 .38979 .38979 .38979 .38979 .38979 .38979 .389799 .38979 .38979 .38979 .38979 .38979 .38979 .38979 .38979 .389799 .38979 .38979 .38979 .38979 .38979 .38979 .38979 .38979 .389799 .38979 .38979 .38979 .38979 .38979 .38979 .38979 .38979 .389799 .38979 .38979 .38979 .38979 .38979 .38979 .38979 .38979 .389799 .38979 .38979 .38979 .38979 .38979 .38979 .38979 .38979 .389799 .38979 .38979 .38979 .38979 .38979 .38979 .38979 .38979 .389799 .38979 .38979 .38979 .38979 .38979 .38979 .38979 .38979 .389799 .38979 .38979 .38979 .38979 .38979 .38979 .38979 .38979 .389799 .38979 .38979 .38979 .38979 .38979 .38979 .38979 .38979 .389799 .38979 .38979 .38979 .38979 .38979 .38979 .38979 .38979 .389799 .38979 .38979 .38979 .38979 .38979 .38979 .38979 .38979 .389799 .38979 .38979 .38979 .38979 .38979 .39979 .39979 .39979 .399799 .39979 .39979 .39979 .39979 .39979 .39979 .39979 .39979 .399799 .39979 .39979 .39979 .39979 .39979 .39979 .39979 .39979 .399799 .39979 .39979 .39979 .39979 .39979 .39979 .39979 .39979 .399799 .39979 .39979 .39979 .39979 .39979 .39979 .39979 .39979 .399799 .39979 .39979 .39979 .39979 .39979 .39979 .39979 .39979 .399799 .39979 .39979 .39979 .39979 .39979 .39979 .39979 .39979 .399799 .39979

<sup>\*</sup>These values were calculated by W. G. Cochran (1934).

### 3.2 Description of the Flow Pattern

In the previous section the general flow equations were deduced for an infinite disk rotating in a semi-infinite fluid. In our special case we want to consider the motion of a limited quantity of liquid flowing on a rotating disk of finite radius. This was done by studying the flow patterns in the layer of the semi-infinite fluid nearest to the disk surface.

The flow on the disk can be described by means of streamlines, that is, the paths which the liquid particles follow as they move radially outwards due to rotation of the disk. In order to characterize the flow as mentioned it is necessary to know the kinematic viscosity of the liquid, the quantity of liquid flowing on to the disk, and the speed of rotation of the disk.

The angular velocity is related to the speed of rotation by the formula  $\omega = \frac{2\pi N}{60} \tag{3.36}$ 

where  $\omega = \text{angular velocity}$ 

N =speed of rotation

Use of formula  $\zeta = z\sqrt{\omega/v}$  (eq. 3.18) enables the determination of the dimensionless distance ( $\zeta$ ) corresponding to an actual distance (z) above the disk (Appendix A). Note that z = 0 corresponds to the surface of the disk. Once the non-dimensionless distance is known, the corresponding velocity functions are obtained from Table 1 and the radial component (u) and tangential component (v) of velocity can be calculated by the relationships  $u = r\omega F(\zeta)$  and  $v = r\omega G(\zeta)$  (eq. 3.20). An example of the resulting velocity profiles obtained is shown in Figure 2.

The area under the velocity distribution curve is proportional to the quantity of liquid flowing through this section. If the thickness of the liquid is known at a given radius then the average radial velocity of the liquid in this layer can be obtained by using the expression

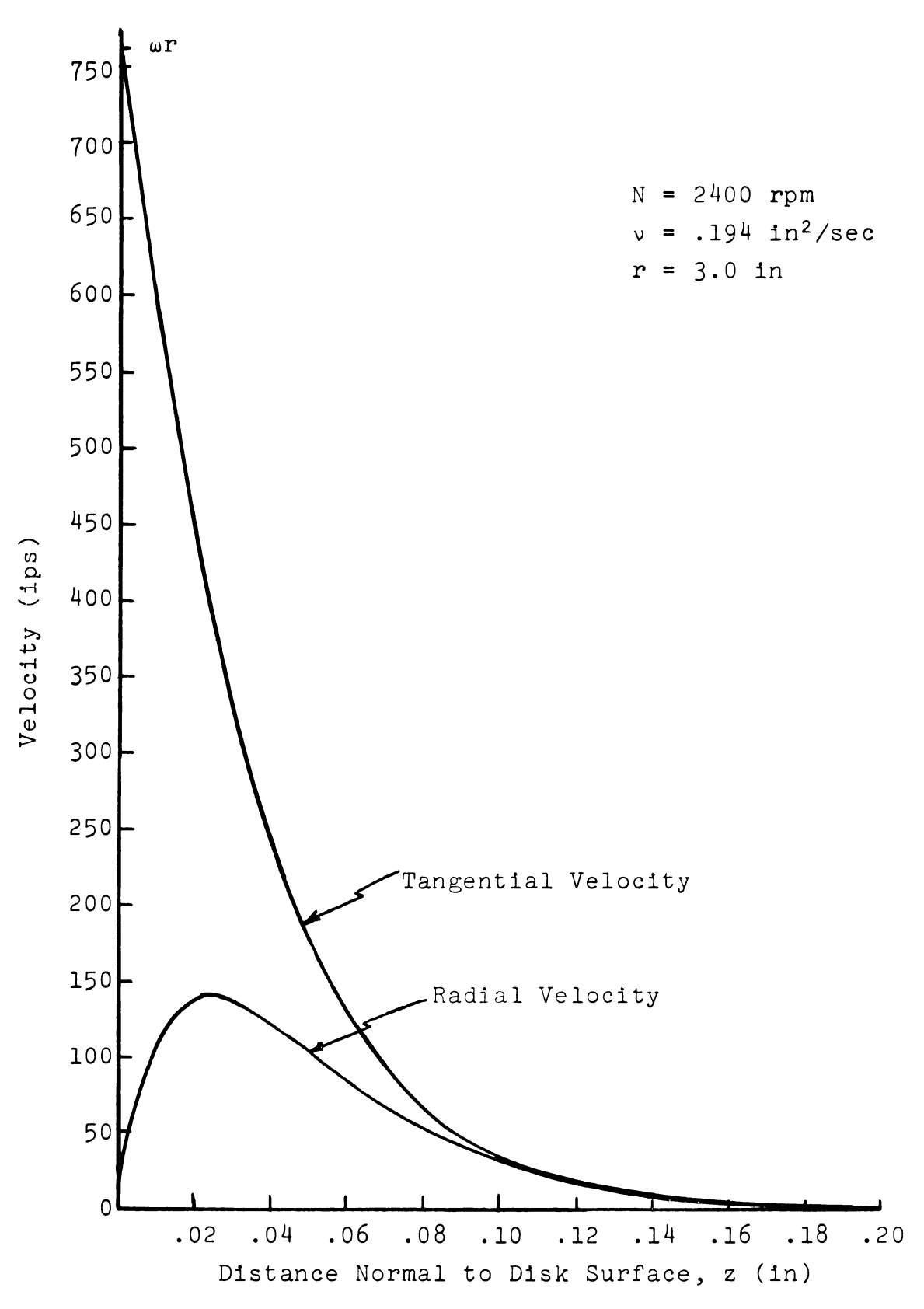


Figure 2. Example of radial and tangential velocity profiles above a rotating disk.

$$u_{A} = \frac{1}{h} \qquad \begin{cases} h & \text{udz} \end{cases}$$
 (3.37)

where  $u_{\Lambda}$  = average radial velocity

h = thickness of liquid

and also the quantity of liquid (Q) flowing on the disk can be calculated by using the expression

$$Q = 2\pi rhu_{\Delta}$$
 (3.38)

The surface of the disk where h=0 represents one streamline. Another streamline can be found by the condition that Q= constant.

The flow between two streamlines in the r-z plane is equal to Q. In our case we were therefore interested in finding this streamline. The values of radial velocity (u) were found numerically and therefore the average radial velocity  $(u_{\Lambda})$  could also only be determined numerically from the graphs of u versus z. The integral (equation 3.37) representing the area under a velocity distribution curve, was evaluated by using a planimeter and applying appropriate scale factors. A trial and error procedure was followed, that is, various h values were selected until the area required under a curve was obtained. After the depth of flow was obtained, the average radial velocity component was determined by using equation 3.37. By determining the h-value at various radii, a streamline (thickness profile) in the r-z plane can be plotted for a given flow rate by assuming constant values of fluid viscosity and rotational speed.

We were also interested in the streamline pattern as seen in the r-0 plane, that is, the direction of motion of particles in the surface z = h. The average tangential velocity component was determined from the tangential velocity distributions by direct use of a planimeter since the depth of flow had already been determined in the determination of the average radial velocity. By considering the geometry of a particle moving from point A to point B as shown in Figure 3 it can be seen that

$$\lim_{\Delta\theta\to0} \frac{1}{r} \frac{\Delta r}{\Delta\theta} = \frac{1}{r} \frac{dr}{d\theta} = \frac{u}{v}$$
 (3.39)

Or this may be written as

$$\frac{d\theta}{dr} = \frac{1}{r} \quad \frac{v}{u} \tag{3.40}$$

The velocity components (u, v) are functions of the radius (r). By plotting the ratio of the velocities v/u, versus radius r (Figure 4) it was observed that there was approximately a linear relationship between this velocity ratio and the radial position along the disk for various flow conditions indicating that a first degree polynomial ought to provide a good approximation for this relationship. Thus assuming  $\frac{v}{u} = Ar + B$  (3.41) where A and B are constants which were calculated for each flow case by the Michigan State University digital computer using library program E2 UTEX LSCFWOP and are shown in Appendix B. Substituting equation 3.41 into equation 3.40

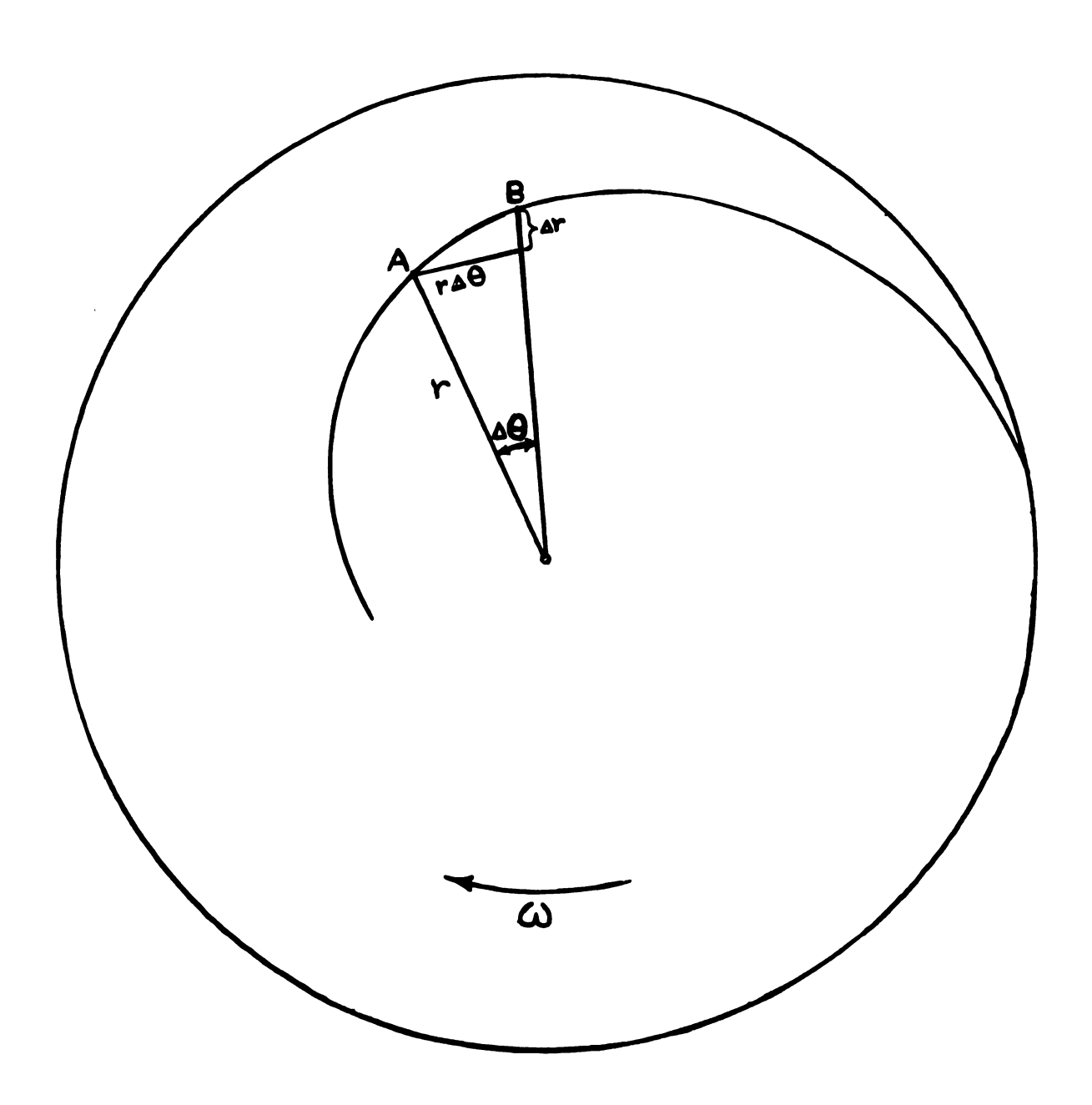


Figure 3. Motion of a particle on a rotating disk.

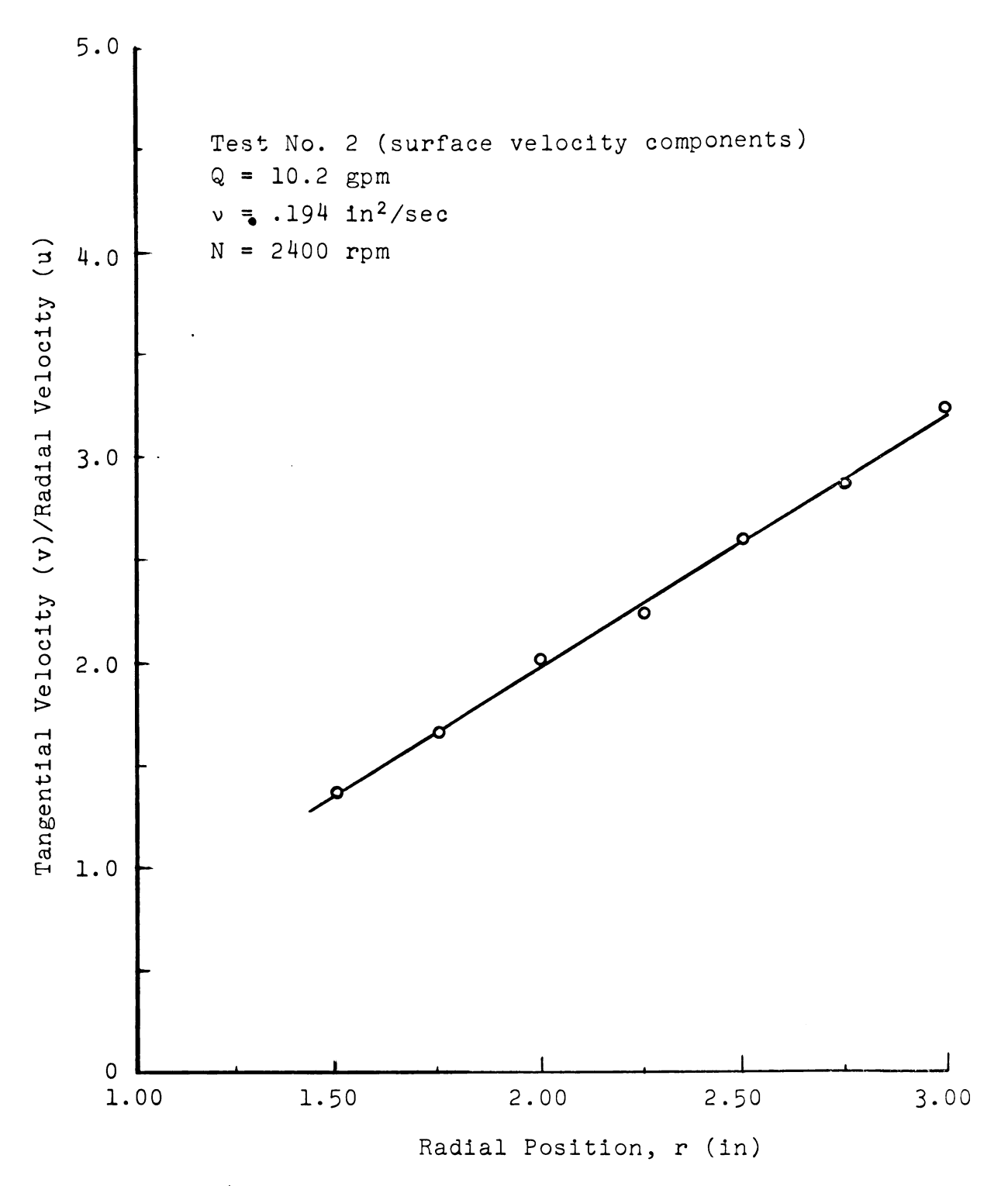


Figure 4. Example of how the ratio of tangential velocity to radial velocity varies with radial position on the disk.

yields the expression

$$\frac{d\theta}{dr} = A + \frac{B}{r} \tag{3.42}$$

By integrating equation 3.42, one obtains the equation

$$\theta = Ar + B \ln r + C \tag{3.43}$$

where C = a constant of integration, which is evaluated by applying an initial condition.

 $\theta$  = angular displacement

Thus by the use of equation 3.43 the curve along which a particle moves can be calculated and the resulting streamline pattern in the  $r-\theta$  plane may be determined (Figure 3). Various streamline patterns will develop at different heights above the disk due to the variations in the magnitudes of the velocity components (u, v). Two streamline patterns in the r-0 plane were plotted for each test considered. One plot was made using the average values of the radial and tangential velocity components at the various radii considered. The other streamline plotted was the one which existed on the surface of this layer. It was found that the term in equation 3.43 which contained the logarithmic function was usually relatively small. Neglecting this term will yield the equation for an Archimedes spiral. Thus a streamline in the r-0 plane approximates an Archimedes spiral.

#### IV. EXPERIMENTAL CONSIDERATIONS

#### 4.1 Description of the Apparatus

An overall view of the testing apparatus is shown in Figure 5. A positive displacement hydraulic pump, powered by an electric motor, supplied liquid to a small reservoir mounted above the rotating disk. The small reservoir was vented near the top to permit oil to flow back to the main reservoir once the liquid reached the level of this opening. This regulated the formation of hydraulic pressure in the system.

The liquid from the small reservoir flowed by gravity through a flow-control valve which was used to vary the liquid flow to the disk. After the liquid passed through the valve it was directed down to the center of the disk through a section of 2-inch (2.0 inch outside diameter and 1.75-inch inside diameter) plexi-glass tubing with its lower edge taped toward the inside. Since it was important to minimize the axial velocity of the liquid as it flowed on to the disk and to keep the tube filled with liquid, metal screens were mounted inside the plexi-glass tube (Figure 6). The number of screens used in the tube depended upon the viscosity of the liquid used. A 3-inch head of liquid was maintained in the tube directly above the disk. Other elements employed in



- Heat lamp
- Main reservoir
- Weight scale
- Dial indicator

- 4. Dial indicator
  5. Thermometer
  6. Plexi-glass tube above disk
  7. Small reservoir
  8. Tachometer
  9. Variable-speed electric moto
- Variable-speed electric motor Hydraulic pump and filter 10.

Figure 5. The testing apparatus.

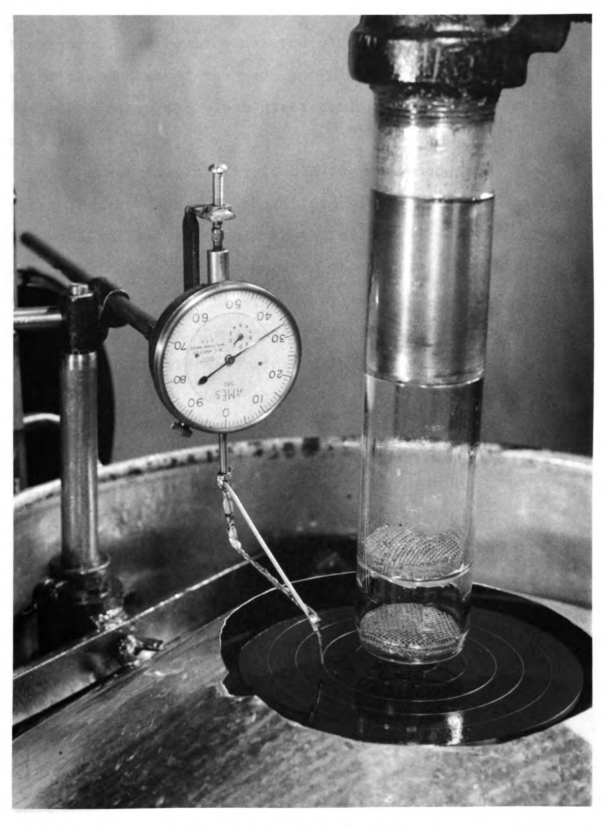


Figure 6. The point gage and plexi-glass tube mounted above the disk.

the hydraulic circuit consisted of a filter mounted directly after the outlet of the pump and a thermometer mounted in the elbow above the plexi-glass tubing for oil temperature measurement.

The quantity of liquid flowing on to the disk was determined by diverting the liquid flowing from the disk into a 1-gallon can placed in the main reservoir (Figure 7). A stop watch was used to measure the time of flow and the amount of liquid was determined by weighing the can with a scale. By knowing the specific gravity of the liquid, the liquid flow (Q) was determined using the relationship

$$Q = \frac{7.20 \text{ W}}{\text{st}} \text{ gpm}$$

where s = specific gravity of the liquid

w = weight of the liquid, lb.

t = time of flow, sec.

A 6-inch diameter steel disk was machined and mounted inside a cylindrical tank (Figure 5). The disk was driven by a variable speed (-3200 rpm to +3200 rpm) electric motor and a 0-2500 rpm tachometer was used to indicate the disk speed. All four legs of the tank and the electric motor were bolted to the concrete floor to reduce vibration.

The thickness of the liquid layer on the disk was measured with an Ames dial indicator, having a range of 0 to 1 inch, graduated in .001 inch increments and accurate to within ±.001 inch, as shown in Figure 6. Initially the

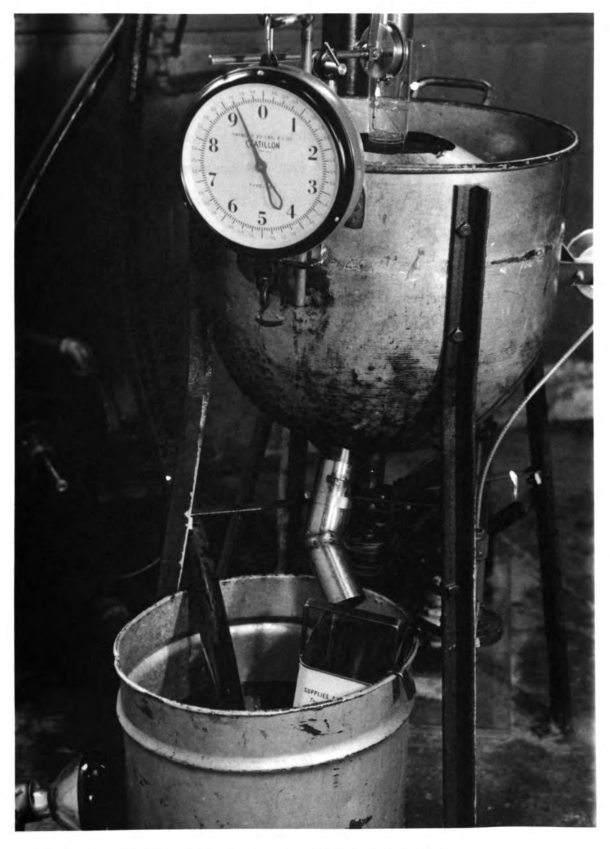


Figure 7. Equipment used for flow measurement.

when the tip of the point gage touched the top surface of the disk. Thus when the pointer was set to just touch the surface of the liquid, the reading on the dial indicator was a direct measurement of the thickness of the liquid flowing. The accuracy of this method of measurement was estimated to be ±.002 inch. The dial indicator was mounted in a support (Figure 6) so that it could be rotated around in a plane parallel to the surface of the disk. Thus the zero reading, representing the surface of the disk, remained the same for every position at which the thickness of the liquid was measured.

#### 4.2 Selection of a Viscous Liquid

The basic requirement of the viscous liquid used in the experimental work is that it be a Newtonian fluid, that is, its viscosity remains constant at any given temperature regardless of the rate of shear. Georgi (1955), Klaus and Fenske (1955), and Appeldoorn et al. (1962) have shown that straight mineral oils behave like Newtonian fluids at temperatures above 32°F. Motor oils which contain appreciable amounts of viscosity index-improving additives were indicated to be non-Newtonian fluids throughout the temperature range to which oils are normally exposed in engines. Because of their suitable properties, straight mineral oils were used in the experimental apparatus to verify the theoretical results.

Two oils were used for the tests: one was an S.A.E. 20 mineral oil (Everest-Cutler Oil Co.) with a typical viscosity of about 300 S.U.S. (Saybolt Universal Seconds) at 100°F and a viscosity index of 45-50; the other oil was an industrial hydraulic oil (Industrial No. 75-American Oil Co.) with a typical viscosity of about 750 S.U.S. at 100°F and a viscosity index of 95-100. Small quantities (20 to 30 parts per million) of silicone foam suppressor (Dow Corning 200 Fluid) were added to both oils to prevent foaming.

#### 4.3 Experimental Procedure

The surface of the disk was sprayed with black paint to provide a dark background for photographing the flow pattern of the liquid. Concentric circles spaced one-half inch apart were drawn on the disk surface to enable a visual determination of radial position on the disk. This facilitated both the method for measuring the thickness of the liquid and the method for studying the streamline pattern on the photographs since the radial positions were clearly marked on the disk and could be observed because the oils used were transparent.

The streamline pattern on the disk was photographed with a single-lense reflex camera (Pentax H-2), with a focal plane shutter, mounted about one foot above the disk. A short extension tube was employed between the lense and the camera body to permit focusing of the lense at shorter

distances. Various shutter speeds were used and it was found that slower shutter speeds of 1/30 sec. or 1/60 sec. were more suitable for obtaining a continuous streamline pattern and the high shutter speeds of 1/250 sec or 1/500 sec. were more suitable for studying the relative velocities of particles as they moved radially outwards.

Since the viscosity of oil is affected by temperature it was necessary to control the operating temperature of the oil during the tests. By operating the experimental apparatus for a period of 2-3 hours it was observed that the temperature of the oil became relatively stable when it reached 95°F. Four 250-watt heat lamps were placed around the oil reservoir to heat the oil to 100°F. The temperature of the oil was then maintained at 100°F (±.2°F) by varying the position and the number of heat lamps as required. All the tests were made employing 6 gallons of oil in the system.

After the equipment had operated for 2 hours with the oil at the operating temperature of 100°F, two samples of the oil were taken for analysis. The specific gravity defined as the weight of a product in relation to the weight of an equal volume of water was determined by the following relationship

specific gravity (s) = weight of the oil
weight of an equal volume of water

Georgi (1950) stated that capillary tube viscosimeters

are considered as the most accurate means available for

Viscosity measurement of lubricating oils. A Series 200 Modified Ostwald Viscosimeter was immersed in a constant temperature bath maintained at 100°F and used for the viscosity determinations. The viscosimeter tube was first calibrated using distilled water as a reference fluid, then the tube was charged with an oil sample. To equalize the liquid temperature with the bath temperature, the liquid was allowed to remain in the tube for 10 minutes before the actual tests were made. The tests consisted of drawing up the liquid sample by suction until the lower bulb was filled and the upper bulb was partially filled. After removing the suction, the liquid was allowed to flow down the tube by gravity and the time is seconds was recorded for the oil level to pass between two etched marks. The kinematic viscosity (v) of the oil sample was determined by using the relationship

$$v = \frac{t}{t_W} v_W$$

 $\nu$  = kinematic viscosity of the oil @100°F

 $v_W$  = kinematic viscosity of the distilled water @100°F

t = time of flow of the oil @100°F

 $t_w = time of flow of the distilled water @100°F$ 

The properties of the oils were determined after the oil was subjected to considerable usage since a small amount of air was entrained in the oil causing the viscosity to

increase slightly and the specific gravity to decrease slightly when compared with the values obtained by employing unused samples. The required properties for the oils are shown in Table 2.

TABLE 2. Values of specific gravity and kinematic viscosity obtained from samples of the oils used in the laboratory tests.

Type of Oil	Specific Gravity (s)	Kinematic Viscosity (ν)in²/sec @100°F
S.A.E. 20 Mineral Oil	.90	.087
Industrial Hydr Oil	aulic .84	.194

The final consideration in the experimental procedure was the determination of what distance should be maintained between the plexi-glass tube and the disk to allow the liquid to flow on to the disk. Preliminary tests indicated that varying this distance from .20 inches to .40 inches produced some variation in the streamline pattern and in the thickness of the liquid only in a region within one-inch from the outside of the tube (radius = 1.0 in) with no noticeable effects produced beyond this region of flow. It was thus decided to maintain a distance of 0.300 inches between the lower taped inside edge of the plexiglass tube and the surface of the disk for all the laboratory tests.

It should be pointed out that it was impossible to duplicate the theoretical flow conditions in the experimental work. The theoretical solution was obtained for the flow of a semi-infinite mass of fluid which could only be expected to be approximately correct for the experimental work where the fluid was a layer of limited thickness.

# V. PRESENTATION AND DISCUSSION OF RESULTS

A series of eight tests were conducted to study the effect of flow rate, viscosity, and rotational speed on the flow of a viscous liquid on a rotating disk. The tests are out-lined in Table 3.

TABLE 3. Tests conducted to study the flow of a viscous liquid on a rotating disk.

Test Number	Kinematic Viscosity (ν) in <sup>2</sup> /sec.	Flow Rate (Q) gpm	Rotational Speed (N) rpm
1	.194	10.2	1000
2	.194	10.2	2400
3	.194	5.0	1000
4	.194	5.0	2400
5	.087	10.2	1000
6	.087	10.2	2400
7	.087	5.0	1000
8	.087	5.0	2400

## 5.1 Streamlines in the r-z Plane

The experimental and theoretical streamlines in the r-z plane (depth of flow versus radial position relationships) are compared in Figures 8 to 11. As was expected, there

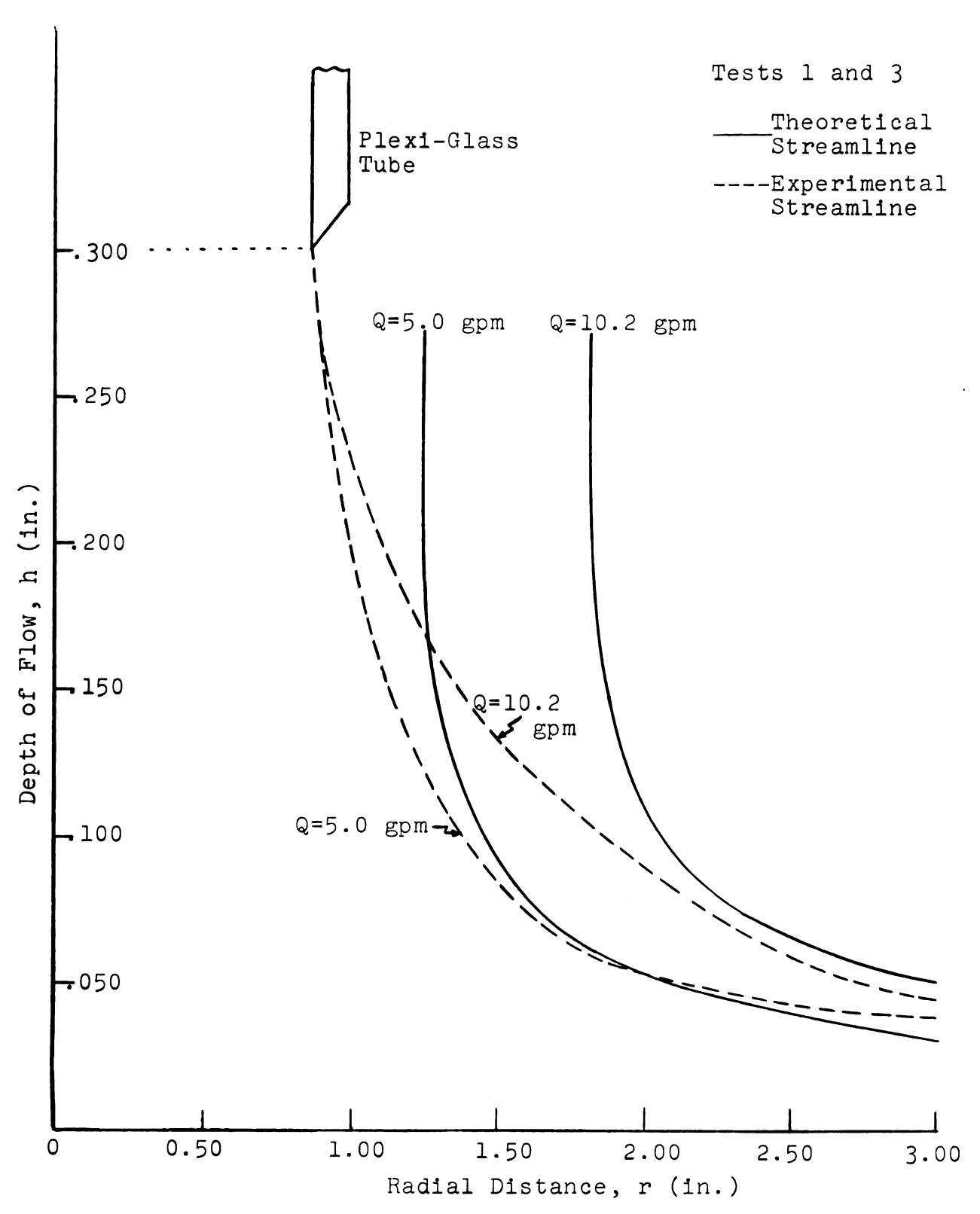


Figure 8. Comparison of experimental and theoretical streamlines in the r-z plane for hydraulic oil ( $v = .194 \text{ in}^2/\text{sec.}$  flowing on a disk rotating at 1000 rpm.

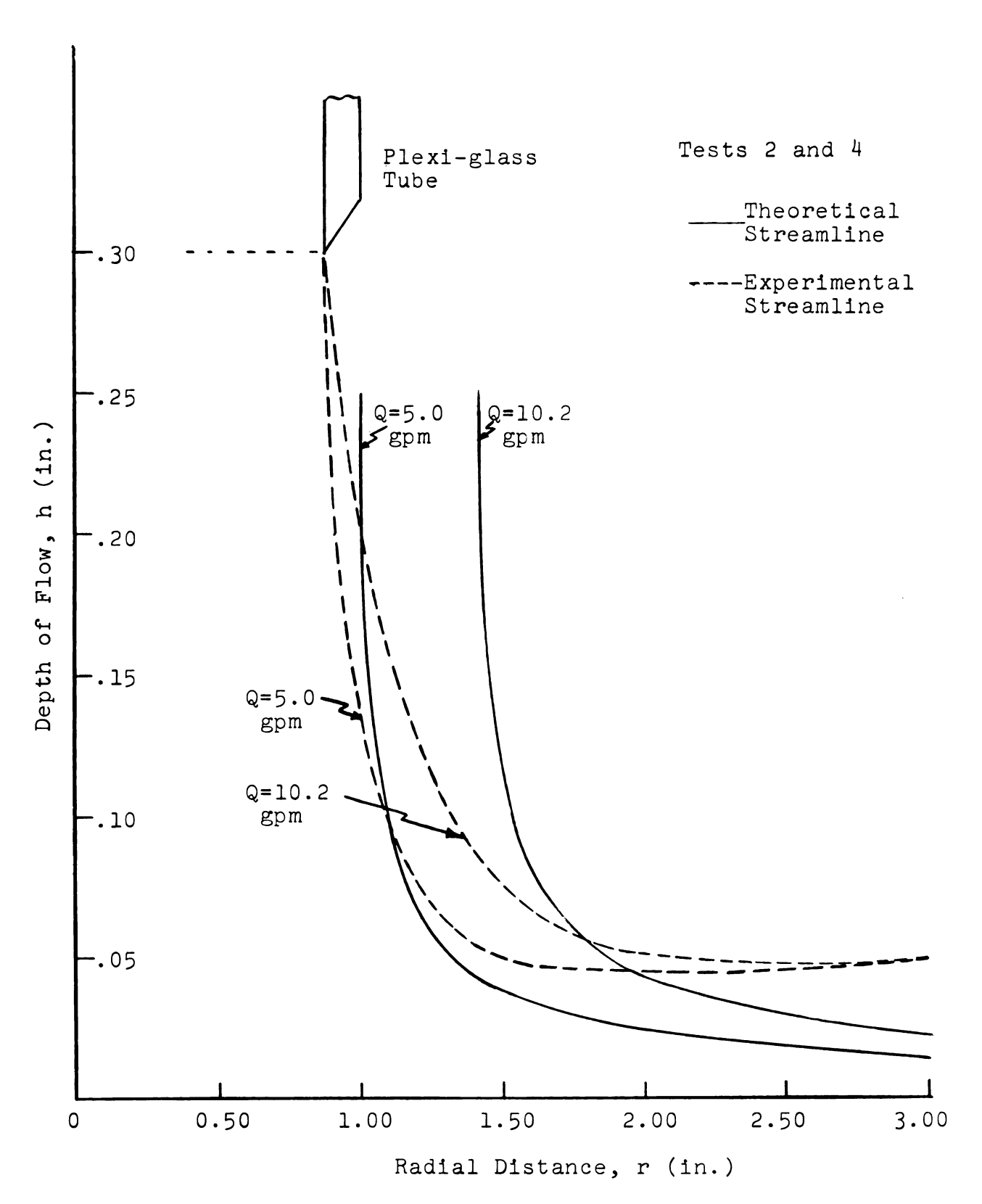


Figure 9. Comparison of experimental and theoretical streamlines in the r-z plane for hydraulic oil ( $\nu$  = .194 in²/sec) flowing on a disk rotating at 2400 rpm.

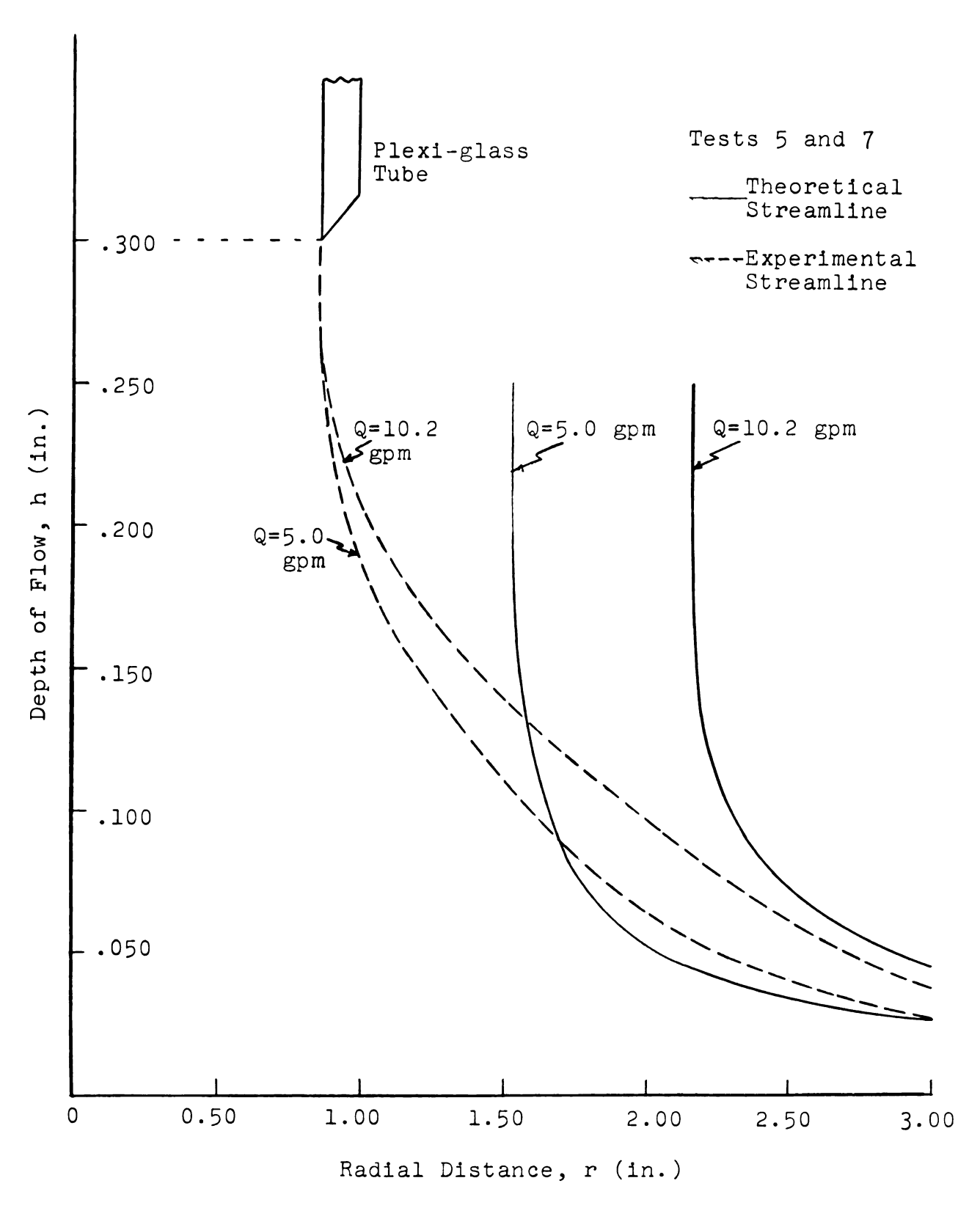


Figure 10. Comparison of experimental and theoretical streamlines in the r-z plane for mineral oil ( $\nu$  = .087 in²/sec) flowing on a disk rotating at 1000 rpm.

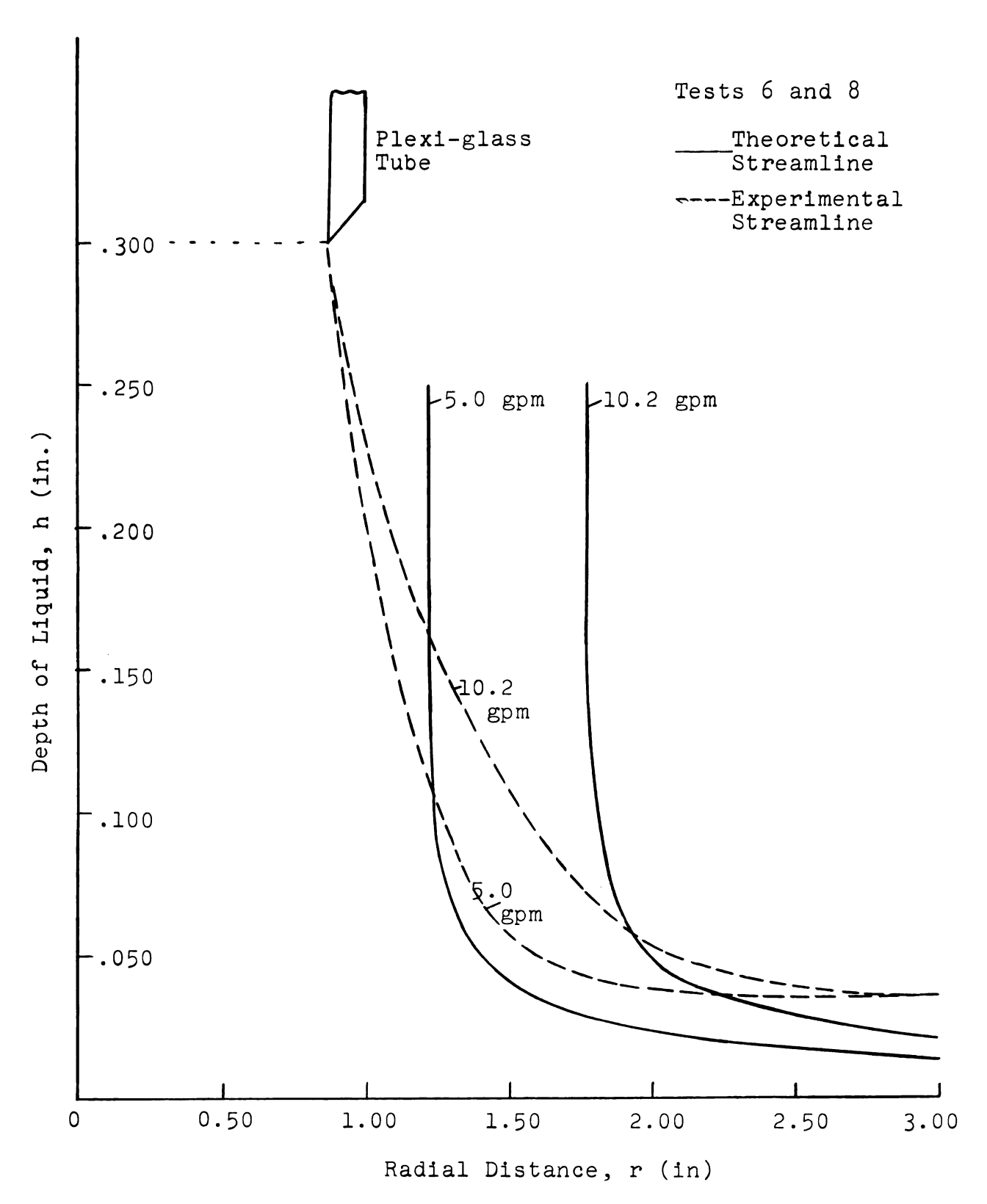


Figure 11. Comparison of experimental and theoretical streamlines in the r-z plane for mineral oil ( $\nu$  = .087 in²/sec) flowing on a disk rotating at 2400 rpm.

was considerable deviation between the experimental and theoretical curves in the area where the oil was initially introduced onto the disk. This was due to the face that in the theoretical solution it was assumed the disk rotated in a body of liquid where there is essentially no point of introduction of the liquid onto the disk. Theoretically however, it is possible as earlier shown to determine a streamline representing a certain flow quantity, assuming constant rotational speed and liquid viscosity. It is interesting to note that theoretically for the velocities and viscosities used in this investigation, a rotating disk has little or no effect on the movement of liquid which is located 0.20 inches or more above the surface of the disk. This is due to the fact that the radial and tangential components of velocity become negligible in this region as shown in Appendix A.

The experimental curves in the area where the oil was introduced onto the disk could have been made to correspond more closely to the theoretical curves by increasing the diameter of the plexi-glass tube, used above the disk, until the inside surface of the tube coincided with the theoretical curve. Increasing the diameter of the tube has the other advantage of reducing the axial velocity of the liquid so as to agree more closely with the theoretical values. In the experimental tests conducted, the axial velocity of the oil at the outlet was usually considerably higher than the theoretical values as shown in Table 4.

TABLE  $\mu$ . Comparison of experimental and theoretical axial velocities at the tube outlet, located .300 inches above the surface of the disk, with the experimental resultant velocity\* at the edge of the disk.

at Tube os	Theoretical Value	4.0 6.1	4.0 6.1	2.6	2.6
Axial Velocity at Outlet (w) ips	Experimental Th Value	16.4 16.4	00.	16.4 16.4	0.0
Experimental	city* at Edge of Disk, ips	205 21 <b>8</b>	147 147	150 210	131 168
	Test No	1 2	M4	62	8
0 + + + + + + + + + + + + + + + + + + +		1000 2400	1000 2400	1000 2400	1000 2400
	Flow Rate (Q) gpm	10.2	5.0	10.2	5.0
Kinematic Viscosity (v) in <sup>2</sup> /sec. (			1	<b>1</b>	000.

\*This velocity was calculated by multiplying the average experimental radial velocity at r = 3 in (Table 7, column 2) by the secant of the surface flow direction relative to the radius (Table 6, column 4).

An increase in the axial velocity of the liquid would tend to increase the resultant velocity of the liquid on the disk. However, since the magnitude of the axial velocity is relatively small compared to the resultant velocity, as shown in Table 4, the difference in the initial kinetic energy may be assumed to have relatively small influence on the final result.

There was good agreement between the experimental and theoretical streamlines at radial distances of two inches or more when the rotational speed of the disk was 1000 rpm (Figures 8 and 10). At the higher rotational speed of 2400 rpm (Figures 9 and 11) the experimental values for the thickness of the liquid were higher than the theoretical values at radial distances of two inches or more. In this flow region it is interesting to note that at the high rotational speed (2400 rpm) the experimental values of depth of flow are affected more by changes in oil viscosity than by changes in the flow rate. In all cases the real influence of flow rate is less than predicted by the theoretical solution. The experimental results also indicated that the boundary layer thickness increased slightly at the edge of the disk at the higher rotational speed rather than decrease as shown by the theoretical values. The variation between the experimental and theoretical curves obtained at the higher rotational speed (2400 rpm) can be at least partially explained by considering boundary-layer stability.

The criteria used to determine the stability of flow is obtained by considering the ratio of inertia forces to friction forces as expressed by the Reynolds number Re. For the case of flow on a rotating disk the value of Re is determined by using the relationship

$$Re = \frac{r^2 \omega}{v} \tag{5.1}$$

where

Re = Reynolds number

r = radial distance

 $\omega$  = angular velocity of the disk

v = kinematic viscosity of the fluid

Schlichting (1960) when considering the torque on a disk rotating in a body of fluid, stated there was good agreement between the theoretical values for laminar flow and the experimental values of torque for Reynolds numbers up to about Re =  $3 \times 10^5$ . At higher Reynolds numbers the flow was definitely turbulent. The curves plotted by Schlichting show that the onset of instability was present at measured Reynolds numbers  $(r^2 \omega/v)$  as low as  $10^4$ . The values of Reynolds numbers present in the experimental tests are summarized in Table 5.

Gregory, Stuart and Walker (1955) discussed boundarylayer instability from both the theoretical and experimental points of view for a disk rotating in a compressible

TABLE 5. Values of Reynolds number present in the laboratory tests.

Kinematic Viscosity (v) in <sup>2</sup> /sec.	Rotational Speed (N) rpm	Test No.	Reynolds r=1.0 in	Number r=2.0 in	(Re) r=3.0 in
.194	1000	1 or 3	.055x104	.22x104	.49x10 <sup>4</sup>
	2400	2 or 4	.13 x10 <sup>4</sup>	.52x10 <sup>4</sup>	1.17x10 <sup>4</sup>
.087	1000	5 or 7	.12 x10 <sup>4</sup>	.48x10 <sup>4</sup>	1.08x10 <sup>4</sup>
.007	2400	6 or 8	.29 x10 <sup>4</sup>	1.16x10 <sup>4</sup>	2.60x10 <sup>4</sup>

fluid (air). They conducted experiments with a 12-inch diameter disk having one side coated with china clay for indicating the transition from laminar to turbulent flow. The boundary-layer velocity profiles were measured and compared with the theoretical laminar profiles. The shapes of some of the curves obtained by Gregory and Walker are shown in Figures 12 and 13. The curves showed that for laminar flow the tangential velocity component was in good agreement with theory, while the radial component had a peak value which is somewhat lower than the theoretical. The experimental profiles (Figures 12 and 13) showed that for turbulent flow both the radial and tangential velocity components had smaller peak values which did not decrease as rapidly as the theoretical values with increasing distance from the disk surface. Gregory et al. stated that on a one-foot diameter disk rotating in air the onset of boundary layer instability occured at Reynolds numbers of  $1.8-2.1 \times 10^5$  and the highest value of Reynolds number at transition,  $2.99 \times 10^5$ , was obtained when the air in the room was at its stillest. The results of this work carried out in an aerodynamic laboratory can be applied to the present investigation on the flow of a viscous liquid (oil) since similar theoretical considerations were made for investigating the boundary layer on the rotating disk. Also it is known that two systems are dynamically similar if their Reynolds numbers are similar.

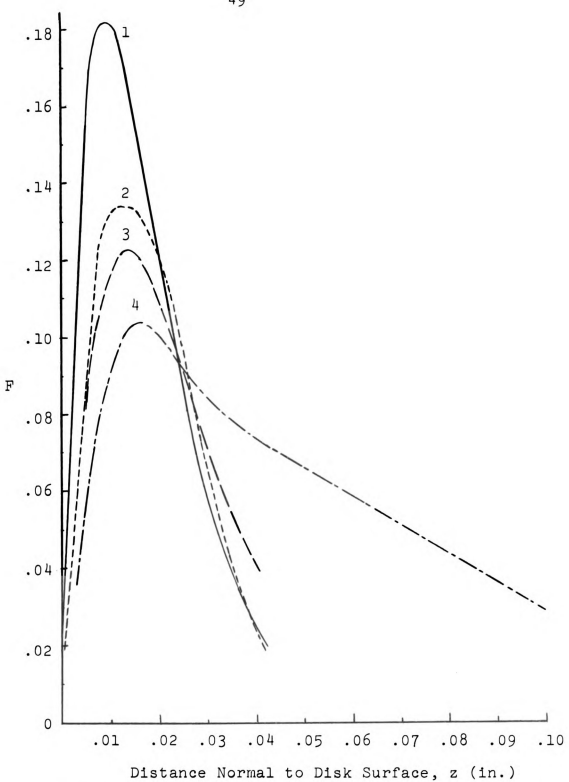


Figure 12. Comparison of experimental and theoretical radial velocity profiles on a disk rotating at 2100 rpm in air (obtained by Gregory et al. 1955). Curve 1, theoretical laminar profile;  $\frac{1}{2}$ ,  $\frac{1}{3}$ , 4 experimental profiles; 2, laminar region; 3, instability region; 4, turbulent region.

Distance Normal to Disk Surface, z (in)

Figure 13. Comparison of experimental and theoretical tangential velocity profiles on a disk rotating at 2100 rpm in air (obtained by Gregory et al. 1955). Curve 1, theoretical laminar profile; 2, 3, 4, experimental profiles: 2, laminar region; 3, instability region; 4, turbulent region.

Thus the variations between the experimental and theoretical curves (Figures 9 and 11) at the higher rotational speed were due to the differences in the shapes of the velocity profiles. At radial distances of two inches or more the experimental values for the thickness of the boundary layer were higher than the theoretical values indicating the actual radial velocity was lower than the theoretical value. This statement is in agreement with the velocity distribution curves (Figure 12) obtained by Gregory et al. The values of Reynolds numbers (Table 5) present in the laboratory tests indicate there was limited turbulent flow present at the higher rotational speed which may have reduced the magnitude of the radial velocity.

It is difficult, however, to explain why the thickness of the liquid, measured at the edge of the disk rotating at 2400 rpm was affected by kinematic viscosity but not by flow rate. In the theoretical consideration it was assumed the disk was an infinite rotating plane. The results were extended to include a disk of finite diameter by neglecting the edge effect. The significance of neglecting the edge effect is not known but it is normally assumed that if the boundary layer thickness is small compared to the radius of the disk then the edge effect can be neglected in a semi-infinite fluid. Since there is a finite quantity of liquid present in our case we must also consider the layer thickness.

The streamlines in the r-0 plane, that is, the path followed by a particle moving on the disk as seen in the direction of the axis, was calculated for two positions in the liquid (Appendix B): the surface streamline was calculated first by using the magnitudes of the velocity components present at the free surface of the liquid and secondly, for comparison, the streamline pattern was calculated using the average values of the radial and tangential velocity components at each radial position considered. A study of the velocity profiles indicated the "average streamline" corresponds approximately to a streamline at two-thirds of the layer height above the disk.

THE REPORT OF THE PERSON AND ADDRESS.

The second secon

The theoretical and experimental streamlines in the r-0 plane are compared in Figures 14 to 21. All the curves are drawn through a common point located two inches from the center of the disk. The experimental curves were approximated by taking measurements from the photographs taken in the laboratory. These experimental curves were assumed to represent the flow on the free surface of the liquid.

Comparison of the experimental and theoretical streamline patterns (Figures 14-21) existing on the surface of the liquid, indicates good agreement especially for cases of high flow (10.2 gpm) and low rotational speeds (1000 rpm). In every case the experimental curve falls between the two

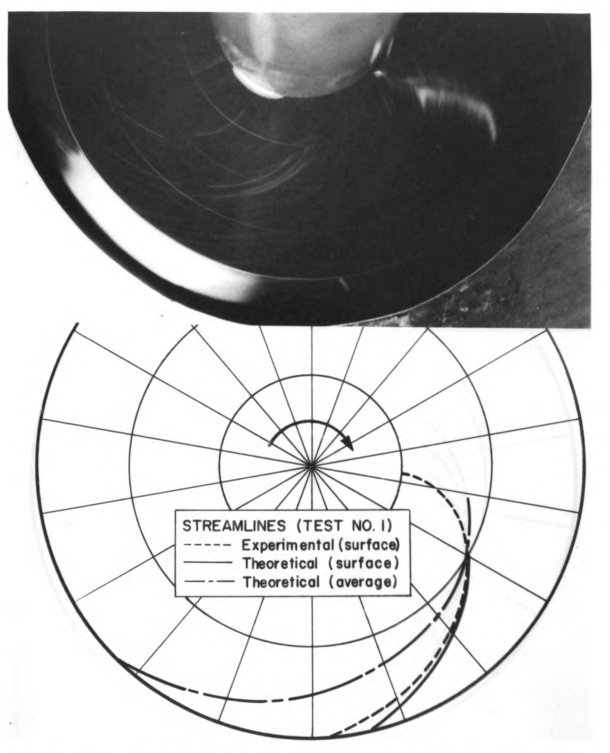


Figure 14. Comparison of experimental and theoretical streamlines in the r-0 plane for 10.2 gpn flow of hydraulic oil (  $_{\nu}$  = .194 in²/sec) onto a disk rotating at 1000 rpm (clockwise) (MSU Photo No. 65772-2).

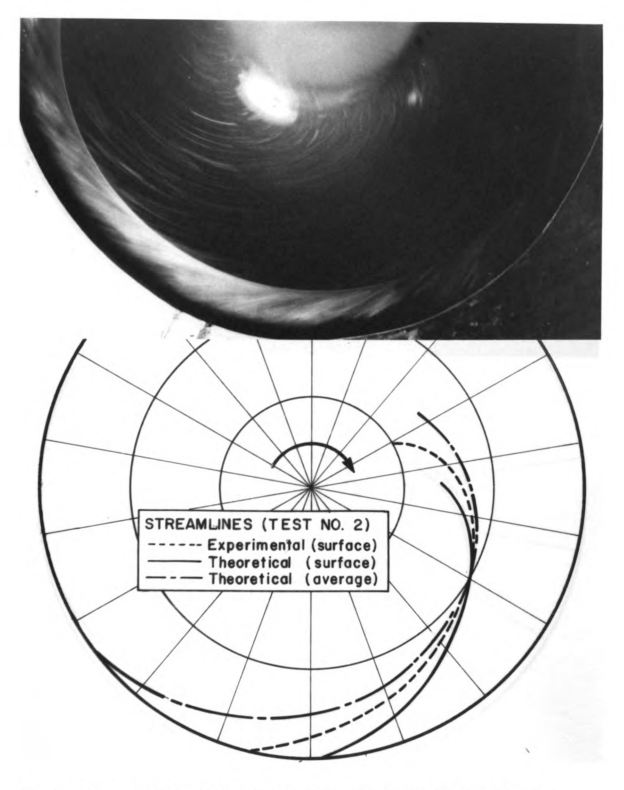


Figure 15. Comparison of experimental and theoretical streamlines in the r-0 plane for 10.2 gpm flow of hydraulic oil ( $\nu$  = .194 in²/sec.) onto a disk rotating at 2400 rpm (clockwise).

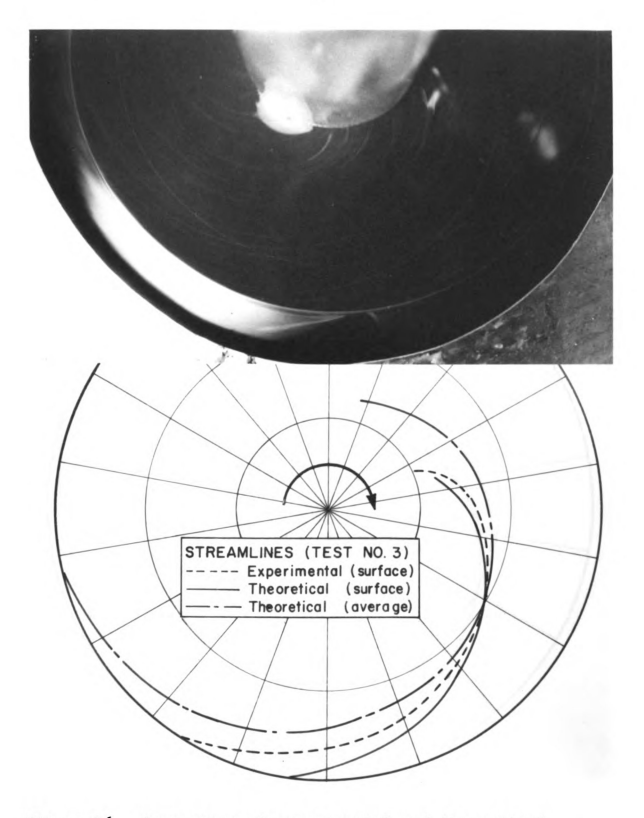


Figure 16. Comparison of experimental and theoretical streamlines in the r-0 plane for 5.0 gpm flow of hydraulic oil ( $\nu$  = .194 in²/sec) onto a disk rotating at 1000 rpm (clockwise).

Figure 17. Comparison of experimental and theoretical streamlines in the  $r_{-\theta}$  plane for 5.0 gpm flow of hydraulic oil (  $_{\nu}$  = .194  $\,$  in 2/sec) onto a disk rotating at 2400 rpm (clockwise) (MSU Photo No. 65772-1).

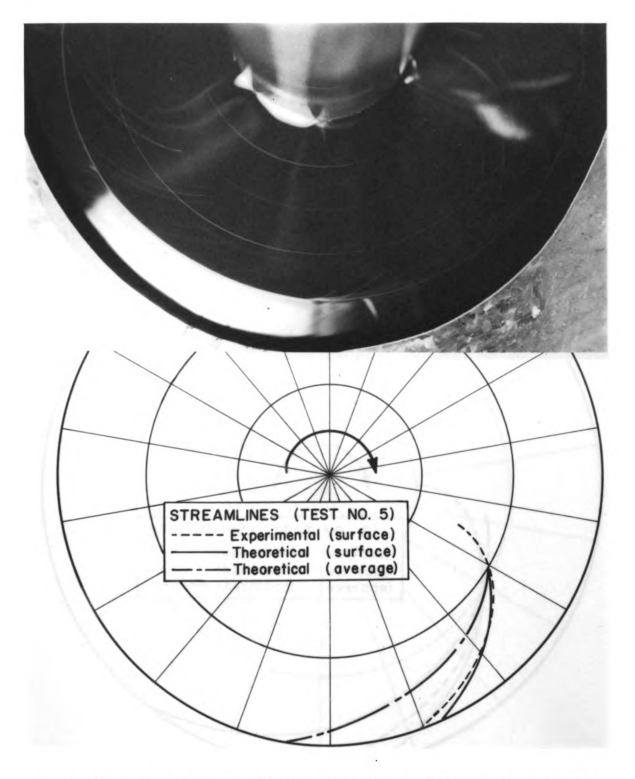


Figure 18. Comparison of experimental and theoretical streamlines in the  $r_{-\theta}$  plane for 10.2 gpm flow of mineral oil ( $\nu$  = .087  $in^2/sec)$  onto a disk rotating at 1000 rpm (clockwise) (MSU Photo No. 65772-5).

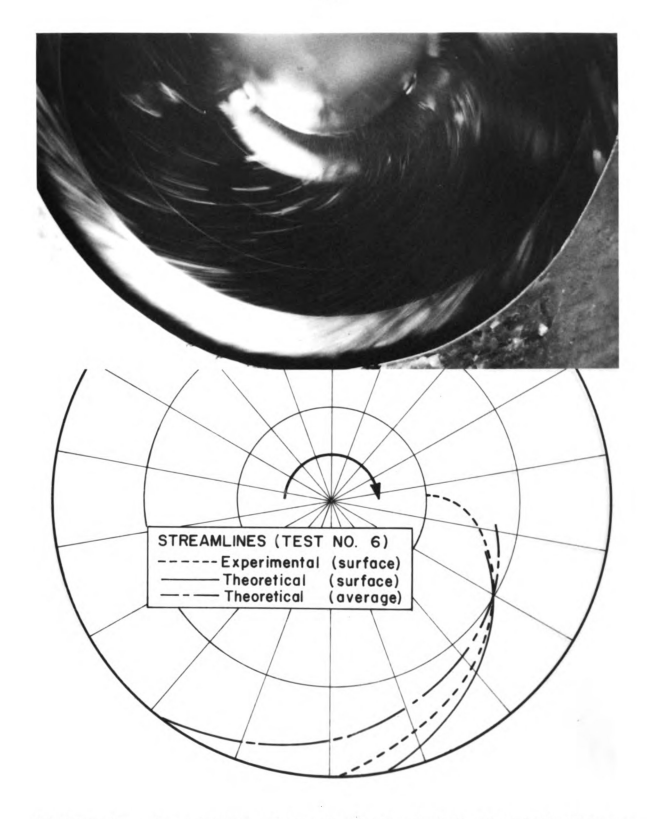


Figure 19. Comparison of experimental and theoretical streamlines in the r-0 plane for 10.2 flow of mineral oil ( $\nu$  = .087 in²/sec) onto a disk rotating at 2400 rpm (clockwise) (MSU Photo No. 65772-6).

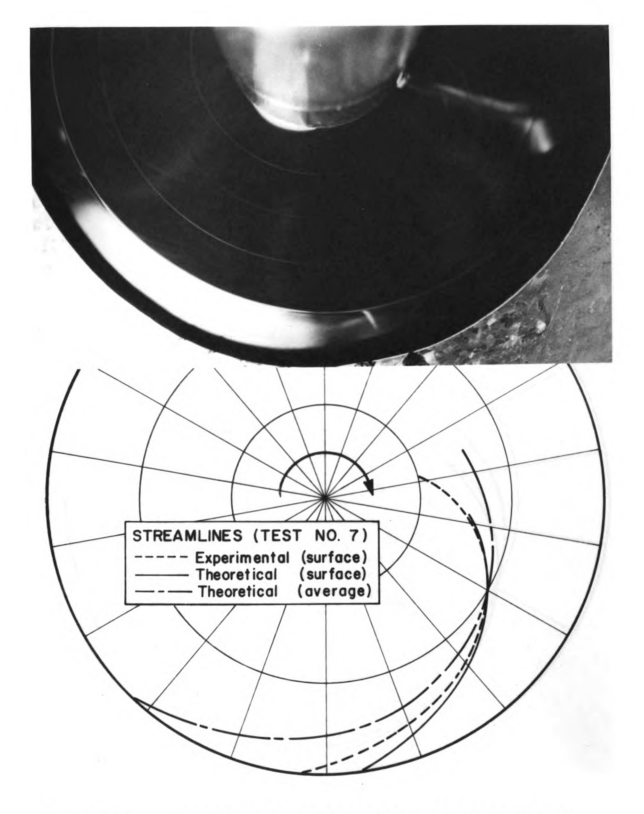


Figure 20. Comparison of experimental and theoretical streamlines in the r-0 plane for 5.0 gpm flow of mineral oil ( $_{\nu}$  = .087 in²/sec) onto a disk rotating at 1000 rpm (clockwise) (MSU Photo No. 65772-7).

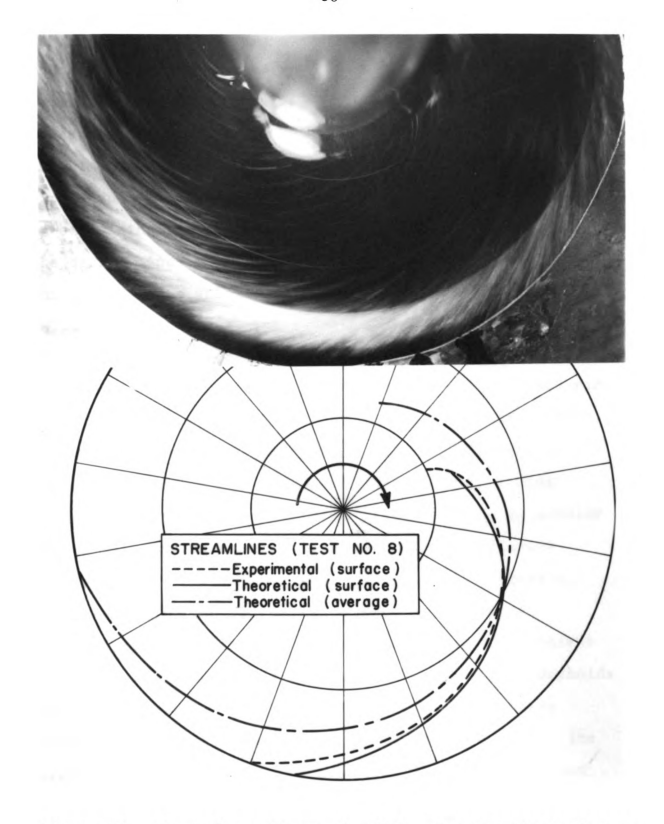


Figure 21. Comparison of experimental and theoretical streamlines in the r-0 plane for 5.0 gpm flow of mineral oil (  $\nu$  = .087 in²/sec) onto a disk rotating at 2400 rpm (clockwise) (MSU Photo No. 65772-8).

theoretical streamline curves: one for surface velocity components and the other for average velocity components at each radial position. The deviations between the experimental and theoretical streamline curves can be explained by a discussion similar to the one given earlier in explaining the variations in the thickness profiles on the disk. Since the radial velocity profile on the disk has a peak value which was smaller than the theoretical value (see Figure 12), the experimental surface streamline fell inside the theoretical curve on the disk. photographs taken at the higher rotational speeds (2400 rpm) did illustrate some transition in the boundary layer near the edge of the disk. Gregory and Walker (1955) took a photograph showing the process of transition on a disk rotating in air. This photograph showed that in an annular region near the edge of the disk there were stationary vortices which assumed the shape of logarithmic spirals. The inner radius of this region marked the onset of instability (Re =  $1.9 \times 10^5$ ) and the transition to turbulent flow occurred at an outer radius corresponding to a Reynolds number of 2.8x10<sup>5</sup>. The values of the Reynolds numbers present in our laboratory tests are shown in Table 5. maximum value of Reynolds number was 2.6xl05 which seemed to indicate that in the present investigation the limit for stability occurred at smaller Reynolds numbers than those indicated by Gregory et al. (1955). It is likely that there was considerable turbulence in the oil as it flowed to the disk through the screens.

The experimental and theoretical surface streamlines are compared in Table 6 by using two descriptive parameters: one was the angular displacement of the particle when moving from a radius of two inches to a radius of three inches (the edge of the disk); the other parameter was the angle relative to the radius with which a particle leaves the disk.

This comparison of the streamlines indicated, in every test, that the experimental values of both the angular displacements and the angles relative to the radius were larger than indicated by the theory.

A final evaluation of the theory was made by comparing the experimental and theoretical average radial and average tangential velocities at the edge of the disk as shown in Table 7. This comparison of the experimental and theoretical velocities indicates relatively good agreement at low rotational speeds (1000 rpm-Tests 1, 3, 5, and 7) but at the high rotational speeds (1000 rpm-Tests, 2, 4, 6, and 8) the theoretical values of velocity were considerably larger than the experimental values.

# 5.3 Flow on Selected Areas of the Rotating Disk

It was mentioned earlier that in certain applications it is desirable to limit the area of liquid flow from a

TABLE 6. Comparison of the experimental and theoretical surface streamlines using angular displacements and angles, relative to the radius, at the edge of the disk.

Experimental Value Theorem 106  106  41  56  66	r=3 in. retical Value 47 59 67 89 36	which particle (degrees typerimental Value 76 79 82 68 74 75	grees)  ue Theoretical Value  69  73  78  65  69  78
	72	80	92

Comparison of the experimental and theoretical average radial and average tangential velocities at the edge of the disk. TABLE 7.

	Velocity at A	verage tanger at edge of	itial velocity disk (ips)	Average radial at edge of di	al velocity disk (1ps)
Test No.	disk at r=3 in, rw(ips)	Expe <b>ri</b> mental Value	Theoretical Value	Experimental Value	Theoretical Value
٦	314	199	218	9.64	41.8
7	751	214	268	41.7	93.3
Μ	314	147	254	25.5	35.5
77	751	145	650	20.4	73.0
5	314	139	188	56.2	45.7
9	751	202	512	57.8	101
7	314	127	227	34.0	39.3
∞	751	166	809	29.2	81.8

rotating disk. An attempt was made to produce a spray pattern similar to the one produced by a fan-type spray nozzle by controlling the introduction of the liquid on to the disk. To produce this form of spray pattern, nozzles with special-shaped openings were constructed to introduce only a sector of the flow normally present with axially-symmetric liquid introduction on to the disk.

The nozzle openings were designed on the basis of the shape of the streamlines existing in the r-0 plane such that the liquid particles at various heights along an edge of the opening would travel out and meet at a common point on the periphery. The horizontal opening between the edges of the nozzle controlled the width of liquid flow from the disk.

Two types of nozzles (Figures 22) were constructed using 3-inch (3.00-inch outside diameter and 2.45-inch inside diameter) plexi-glass tubing: one nozzle had a closed bottom which permitted liquid to flow out through an opening in the side, the other nozzle had an open bottom which permitted liquid to flow against the disk within the nozzle. Both nozzles had parallelogram-shaped openings (Figure 23) designed on the basis of the theoretical streamlines in the r-0 plane from r=1.5 in (outside of the nozzle) to r=3 in (edge of the disk) as shown in Figure 23. The slope of the edges of the openings was determined by measuring the angular distance between the surface

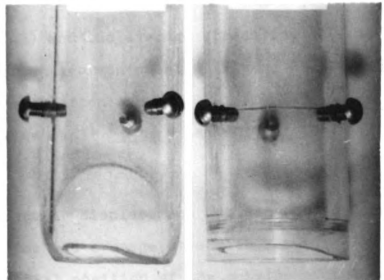


Figure 22. Closed-bottom nozzle (left) and open-bottom nozzle (right) with parallelogram shaped openings.

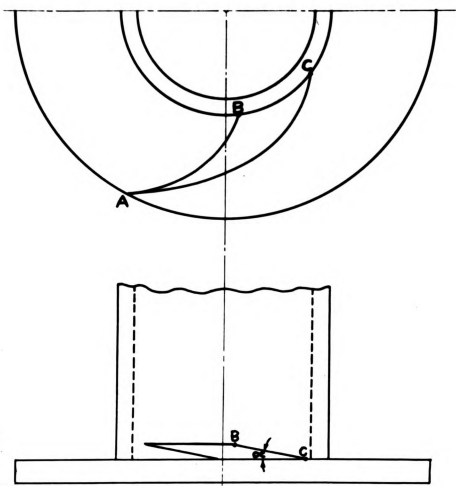


Figure 23. Diagram of a parallelogram-shaped nozzle opening.

streamline (AB) and the average streamline (AC) at r=1.5 in. when drawn from a common point A (Figure 23) at r=3.0 in. and using the relationship

Slope (
$$\langle \rangle$$
) =  $\tan^{-1} \frac{\mathbf{r}_1 \theta_1}{h}$  =  $\tan^{-1} \frac{1.5 \theta_1}{h}$ 

where

 $\theta_1$  = angular displacement between the surface streamline and average streamline at  $r_1$ 

 $r_1$  = radial position of the outside of the nozzle

h = depth of the liquid

Calculations based on the methods presented earlier (section 3.2) showed that the "average streamline" corresponded to the particle movement at from approximately one-third to two-thirds of the layer height above the disk. Thus in the present design considerations the streamlines corresponding to particle movement at less than one-third of the layer depth were not considered. The amount of radial flow in this bottom layer is, however, small. A liquid depth of .20 inches was selected for the nozzle design. The horizontal distance between the sloping edges of the nozzle opening corresponded to an angular displacement of approximately 75 degrees, representing a typical spray width for a hydraulic spray nozzle. By varying the flow rate, a 7-inch head of hydraulic oil ( $v = 194 \text{ in}^2/\text{sec.}$ ) was maintained above the nozzle opening in all the tests.

The flow patterns from the special nozzles are shown in Figures 24 to 27. A rotational speed of 1000 rpm was employed for these tests since it was observed that increasing the speed to 2000 rpm had little noticeable effect on the flow pattern. The resulting flow patterns indicate the presence of high tangential velocity and low radial velocity of the liquid closest to the disk. In Figure 27 a large air bubble is clearly visible along the outside of the nozzle which shows that the calculated angular displacement of the layers at the inlet to the disk was as desired.

After measuring both the depth of the oil and the resultant flow direction and by assuming a uniform velocity profile in the liquid at the edge of the disk the proportion of oil leaving the disk at various areas was determined. On the basis of these results it was observed that in the area of highest concentration approximately two-thirds of the liquid was leaving the disk in one-fifth of the circumference. It is felt that with further work and the addition of shrouds to prevent the undesirable flow, the disk may be used to produce an acceptable fan-type spray pattern.

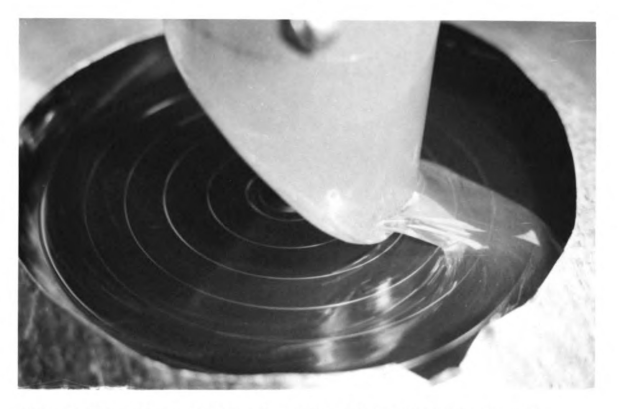


Figure 24. Flow pattern from the closed-bottom nozzle (N = 1000 rpm, Q = 4.4 gpm, $\nu$  = .194 in<sup>2</sup>/sec.).

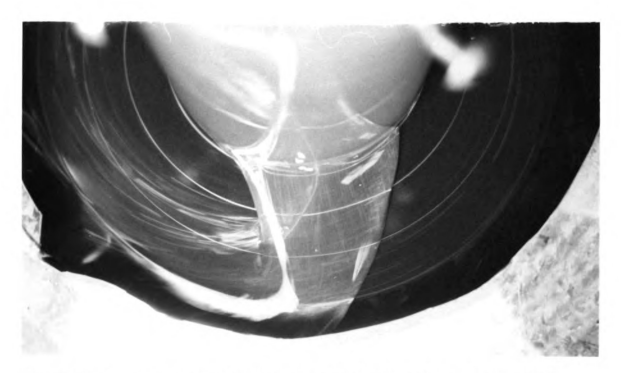


Figure 25. Streamlines in the r-0 plane for the closed-bottom nozzle (N = 1000 rpm, Q = 4.4 gpm  $\nu$  = .194 in²/ sec.).

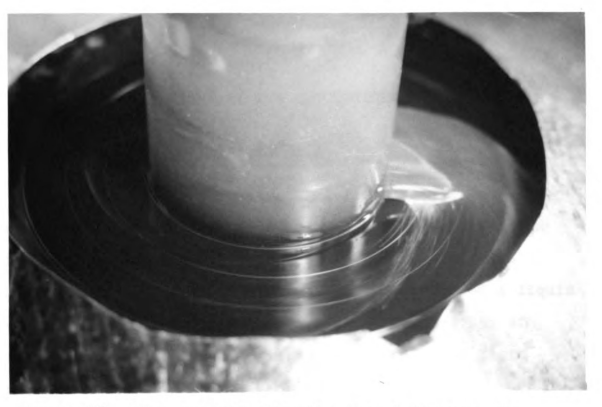


Figure 26. Flow pattern from the open-bottom nozzle (N = 1000 rpm, Q = 5.4 gpm,  $\nu$  = .194 in  $^2$  /sec) (MSU Photo No. 65772-15).

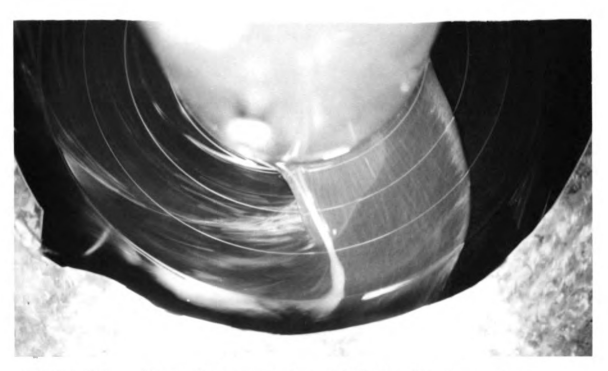


Figure 27. Streamlines in the r-0plane for the openbottom nozzle (N - 1000 rpm, Q = 5.4 gpm,  $\nu$  = .194 in  $^2$  /sec) (MSU Photo No. 65772-16).

#### VI. SUMMARY AND CONCLUSIONS

## 6.1 Summary

The principle of centrifugal distribution or atomization of liquids has many inherent advantages. An investigation was conducted to obtain a more thorough understanding of the factors affecting the flow of a liquid on a rotating disk and to determine the feasibility of using theoretical considerations to describe the fluid motion.

In this investigation a solution to the Navier-Stokes equations, for the case of flow around a disk rotating in a fluid at rest, was applied to the present flow situation. The flow on the disk was characterized by means of streamlines in both the r-0 plane and the r-z plane. In order to obtain the thickness profile for a specified flow condition, the areas under the velocity profiles were found with a planimeter. A first order polynomial approximation for the ratio of tangential velocity to radial velocity as a function of radius was integrated and used to obtain an equation for the path traced by a particle moving on the disk.

An experimental apparatus consisting of a 6-inch (15.2 cm) diameter steel disk powered by a variable-speed

The thickness of the oil layer on the disk was measured with a point gage and the surface streamline patterns in the  $r-\theta$  plane were obtained from a photograph. The theoretical and experimental curves were compared and the deviations between some of the curves were explained.

WELL CHERT THE THE PROPERTY ALL SAME

Preliminary experiments were made injecting liquid through special nozzles on a section of the disk.

## 6.2 Conclusions

As a result of this study, the following conclusions are presented:

- 1. The Navier-Stokes flow equation can be successfully used to predict the laminar flow of a Newtonian fluid on a rotating disk. The actual deviations from the theoretical solution are discussed below in point 6.
- 2. Increasing the kinematic viscosity of the liquid increased the boundary layer thickness of the liquid on the disk and also increased the angular displacement of the liquid on the disk which resulted in a higher resultant average velocity of the liquid leaving the edge of the disk, assuming constant flow rate and rotational speed.
- 3. Increasing the flow rate of the liquid onto the disk increased the boundary layer thickness of the liquid on the disk and also decreased the angular displacement of the liquid on the disk which resulted in a lower resultant average velocity of the liquid leaving the edge of the disk, assuming constant liquid viscosity and rotational speed.

- 4. Increasing the rotational speed of the disk decreased the boundary layer thickness of the fluid on the disk and also increased the angular displacement of the liquid on the disk which resulted in a higher resultant average velocity of the liquid leaving the edge of the disk, assuming constant liquid viscosity and flow rate.
- 5. The angle relative to the radius with which a liquid particle leaves the disk increases with increased angular displacement of the liquid, increased disk radius and decreased height above the disk surface. This angle has a maximum value of 90 degrees on the surface of the disk implying that a particle at this height has only tangential velocity. As the distance above the disk increases the flow becomes more in a radial direction.
- 6. When compared with the theoretical results, the experimental results indicated that the flow rate had less effect than theoretically expected, while the viscosity and the rotational speed had the expected effect on the streamlines used to characterize the liquid flow on a rotating disk. Comparison of the surface streamlines in the r-θ plane indicated that in every test the

- experimental values of both the angular displacements and the angles relative to the radius were slightly larger than indicated by the theory.
- 7. When the liquid was introduced axially symmetrical onto the rotating disk, the liquid was uniformly distributed about the entire periphery of the disk. By introducing the liquid through a special-shaped nozzle on a section of the disk, approximately two-thirds of the liquid left the disk on one-fifth of the circumference of the disk.

### SUGGESTION FOR FURTHER STUDY

Further investigations should be conducted to obtain a better understanding in the following areas:

- 1. Edge Effect.--Tests should be conducted with disks having various diameters so that the edge effect of the disk can be determined.
- 2. <u>Velocity Profiles.</u>—Instrumentation should be employed to enable measurement of the velocity components at different positions in the liquid.
- 3. <u>Liquid Introduction</u>. -- The diameter of the tube used to introduce the liquid onto the disk should be varied to satisfy the conditions dictated by the theoretical solutions.
- 4. Partial Flow. -- More extensive laboratory tests should be conducted with special shaped nozzles and auxiliary devices should be added to provide better control of the liquid flow.

#### REFERENCES

- Appeldoorn, J. K., Okrent, E. H., and Philippoff, W. 1962 Viscosity and elasticity at high pressures and high shear rates. American Petroleum Institute Proceedings, Section III Vol. 42:163-172.
- Bainer R., Kepner, R. A., and Barger, E. L.
  1955 Principles of Farm Machinery. John Wiley and
  Sons Inc., New York 571 pp.
- Bödewadt, U. T.

  1940 Die Drehströmung über festem Grunde. Zeitschrift
  Für Angewandte Mathematik Und Meckanik. Vol. 20:
  241-253.
- Cochran, W. G.
  1934 The flow due to a rotating disc. Cambridge
  Philosophical Society Proceedings. 30:365-375.
- Crowther, A. J.

  1958 The distribution of particles by a spinning disc.

  Journal of Agricultural Engineering Research

  3 (4):288-291.
- Fettis, H. E.

  1955 On the integration of a class of differential equations occuring in boundary layer and other hydrodynamic problems. Proceeding of 4th Midwestern Conference on Fluid Mechanics: 93-114
- Georgi, C. W.
  1950 Motor Oils and Engine Lubrication, Reinhold
  Publishing Corporation, New York: 514 pp.
- Georgi, C. W.
  1955 Viscosity characteristics of motor oils at higher shear rates. Proceedings Fourth World Petroleum Congress, Rome. Section VI/C: 211-221.
- Gregory, N., Stuart, J. T., and Walker, W. S.

  On the stability of three-dimensional boundary layers with application to the flow due to a rotating disk. Royal Society of London Philosophical Transactions A248:155-199.

- Gunkel, W. W.
  - Deposit of mist concentrate spray as influenced by droplet size, air velocity, temperature and humidity. Thesis for the degree Ph.D, Michigan State University, East Lansing. (unpublished)
- Hannah, D. M.
  - 1947 Forced flow against a rotating disc. Great Britain Aeronautical Research Council Reports and Memoranda No 2772:1-17.
- Homann, Von F.
  - 1936 Der Einfluss grosser Zähigkeit bei der Strömung um den Zylinder und um die Kugel. Zeitschrift Für Angewandte Mathematik Und Mechanik. Vol. 16, No. 3: 153-164.
- Houghton, H. G.
  - Spray Nozzle. pp 1170-1175 Chemical Engineers Handbook, third edition. John H. Perry, editor. McGraw-Hill Book Co. New York, pp. 1170-1175.
- Inns, F. M., and Reece, A. R.
  - 1962 The theory of the centrifugal distributer (II), Journal of Agricultural Engineering Research 7(4): 345-353.
- Kármán, Th...von
  - 1921 Uber laminare und tubulente Reibung. Zeitschrift Für Angewandte Mathematik Und Mechanik. Vol. 1, No. 4: 233-252.
- Kármán, Th. and Lin, C. C.
  - 1961 On the existence of an exact solution of the equations of Navier-Stokes. Communications on Pure and Applied Mathematics 14: 645-655.
- Klaus, E. E. and Fenske, M. R.
- 1955 Some viscosity-shear characteristics of lubricants. Lubrication Engineering, March-April: 101-108.
- Lance, G. N., and Rogers, M. H.
- 1962 The axially symmetric flow of a viscous fluid between two infinite rotating disks. Royal Society Proceedings 266: 109-121.
- Leigh, D. C.
- 1955 The laminar boundary-layer equation: a method of solution by means of an automatic computer. Cambridge Philosophical Society Proceedings 51; 320-332.

- Patterson, D. E. and Reece, A. R.

  1962 The theory of the centrifugal distributor (I).

  Journal of Agricultural Engineering Research
  7(3): 232-240.
- Schlichting, Von H. and Truckenbrodt, E.

  1952 Die Strömung an einer angeblasenen rotierenden
  Schiebe. Zeitschrift Für Angewandte Mathematik
  Und Mechanik Vol. 32: 97-111.
- Schlichting, Von H.
  1960 Boundary Layer Theory. McGraw-Hill, Inc.,
  New York. 647 pp.
- Stewartson, K.

  1952 The flow between two rotating coaxial disks.

  Cambridge Philosophical Society Proceedings. 49:
  333-341.
- Stuart, J. T.

  1954 On the effects of uniform suction on the steady flow due to a rotating disk. Quarterly Journal Mechanics and Applied Mathematics 7:446-457
- Truckenbrodt, E.

  1954 Die turbulente Strömung an einer angeblasenen rotierender Scheibe. Zeitschrift Für Angewandte Mathematik Und Mechanik Vol. 34: 150-162.
- Rogers, M. H. and Lance, G. N.
  1960 The rotationally symmetric flow of a viscous fluid in the presence of an infinite rotating disk. Journal of Fluid Mechanics 7: 617-631.
- Tifford, A. N. and Chu, Sheng To
  1952 On the flow around a rotating disc in a uniform stream. Journal Aeron. Sciences Readers Forum
  19: 284.
- Wu, J. C.

  1961 On the finite difference solution of laminar boundary layer problems. Proceedings of Heat Transfer and Fluid Mechanics Institute, Stanford, California: 55-69.
- Yates, W. E.

  1951 An analysis of atomization by the rotating disk for controlled droplet size. Unpublished thesis, University of California.

APPENDIX A

TABLE A1. Dimensionless radial (F) and tangential (G) velocity components for hydraulic oil ( $_{\rm v}$  = .194 in  $^2/{\rm sec.}$ ) flowing on a disk rotating at both 1000 rpm

·	N = 1000  rpm			N = 2400  rpm	
2	Ēυ	G	V	ÎΞ	ტ
=23.24z	(radial)	(tangential)	=36.02z	(radial)	(tangential)
•		00.	•	•	00.
9		0.9287	0	077	0.8895
.232	1.094	.858	.360	.128	.783
794.	1.147	.726	.720	.175	.597
•		.60	•	•	44
.929	.180	.505	044.	.159	.329
.162	.175	.416	.801	.133	.241
.394	.162	.342	.161	901.	176
.626	.146	.281	.521	.083	.128
.859	.129	.229	.881	.063	.092
.091	1111	.187	.241	.047	.067
.324	.095	.153	.602	.035	.048
.556	.081	.124	.962	.026	.034
.788	1.067	.100	.322	.019	.024
.021	.056	.081	.682	.014	.017
.253	.047	990.	.042	.010	.012
. 486	.039	.053	.403	.007	.008
.718	.032	.043	.763	.005	.005
.950	.026	.035	.123	.003	.003
.183	.021	.028	. 483	.002	.001
.415	.017	.022	.843	.001	.000
879	700	α [ ر	204	רככ	

TABLE A2. Radial velocity components for hydraulic oil ( $\nu$  = .194 in<sup>2</sup>/sec.) flowing on a disk rotating at 1000 rpm.

Z			Velocity (in		
(in)	r=1.0 in	r=1.5 in	r=2.0 in	r=2.5 in	r=3.0 in
0.0	0.0	0.0	0.0	0.0	0.0
0.005	5.52	8.28	11.04	13.79	16.56
0.01	9.84	14.76	19.68	24.60	29.53
0.02	15.49	23.23	30.97	38.71	46.46
0.03	18.20	27.30	36.39	45.59	54.60
0.04	18.90	28.36	37.80	47.25	56.71
0.05	18.34	2 <b>7.</b> 52	36.69	45.86	55.04
0.06	17.02	25.54	34.04	42.56	51.08
0.07	15.36	23.04	30.72	38.40	46.09
0.08	13.51	20.26	27.01	33.77	40.53
0.09	11.71	17.56	23.41	29.26	35.12
0.10	10.04	15.06	20.08	25.10	30.13
0.11	8.48	12.72	16.96	21.20	25.45
0.13	5.95	8.92	11.89	14.87	17.84
0.14	4.93	7.40	9.86	12.33	14.80
0.15	4.08	6.12	8.17	10.21	12.25
0.16	3.37	5.06	674	8.43	10.12
0.17	2.76	4.15	5.53	6.91	8.29
0.18	2.27	3.41	4.54	5.68	6.82
0.19	1.85	2.78	3.71	4.63	5.56
0.20	1.52	2.28	3.04	3.80	4.56

TABLE A3. Tangential velocity components for hydraulic oil ( $\nu$  = .194 in²/sec.) flowing on a disk rotating at 1000 rpm.

z (in)	r=1.0 in	Tangential r=1.5 in	Velocity (	_	r=3.0 in
0.0	104.72	157.08	209.44	261.80	314.16
0.005	97.25	145.88	194.51	243.13	291.76
0.01	89.91	134.87	179.83	224.78	269.74
0.02	76.08	114.12	152.16	190.20	228.24
0.03	63.67	95.50	127.34	159.17	191.01
0.04	52.88	79.33	105.77	132.21	158.65
0.05	43.59	65.39	87.19	108.99	130.78
0.06	35.86	53.78	71.71	89.64	107.57
0.07	29.47	44.20	58.94	73.67	88.40
0.08	24.02	36.03	48.05	60.06	72.07
0.09	19.59	29.39	39.19	48.98	58.78
0.10	16.02	24.03	32.04	40.06	48.07
0.11	13.00	19.49	25.99	32.49	38.99
0.12	10.57	15.85	21.13	26.42	31.70
0.13	8.58	12.86	17.15	21.44	25.73
0.14	6.93	10.40	13.86	17.33	20.80
0.15	5.63	8.45	11.27	14.08	16.90
0.16	4.56	6.83	9.11	11.39	13.67
0.17	3.68	5.51	7.35	9.19	11.03
0.18	2.95	4.43	5.91	7.38	8.86
0.19	2.37	3.55	4.73	5.92	7.10
0.20	1.90	2.84	3.79	4.74	5.69

TABLE A4. Radial velocity components for hydraulic oil ( $\nu$  = .194 in<sup>2</sup>/sec.) flowing on a disk rotating at 2400 rpm.

z		Radial V	elocity (ips	s) u=rωF	
(in)	r=1.0 in	r=1.5 in	<b>r=</b> 2.0 in	r=2.5 in	r=3.0 in
0.0	0.0	0.0	0.0	0.0	0.00
0.005	19.38	29.07	38.76	48.44	57.90
0.01	32.22	48.33	64.44	80.55	96.28
0.02	44.03	66.05	88.07	110.08	131.57
0.03	44.73	67.10	89.47	111.84	133.68
0.04	40.11	60.17	80.22	100.28	119.86
0.05	33.52	50.29	67.05	83.83	100.18
0.06	26.86	40.30	53.73	67.17	80.28
0.07	20.88	31.33	41.77	52.21	62.41
0.08	15.91	23.86	31.82	39.77	47.54
0.09	11.96	17.94	23.93	29 <b>.9</b> 1	35.75
0.10	8.92	13.38	17.84	22.31	26.66
0.11	6.58	9.88	13.17	16.46	19.68
0.12	4.82	7.24	9.65	12.06	14.42
0.13	<b>3.</b> 52	5.28	7.04	8.80	10.51
0.14	2.56	3.85	5.13	6.41	7.66
0.15	1.86	2.79	3.72	4.65	5.56
0.16	1.36	2.04	2.71	3.39	4.06
0.17	•95	1.43	1.91	2.39	2.85
0.18	.68	1.02	1.36	1.70	2.03
0.19	.48	.72	.96	1.19	1.43
0.20	.34	.51	.68	0.85	1.01

TABLE A5. Tangential velocity components for hydraulic oil ( $\nu$  = .194 in²/sec.) flowing on a disk rotating at 2400 rpm.

z		Tangential	Velocity (in	os) v=rωG	
(in)	r=1.0 in	r=1.5 in	r=2.0 in	r=2.5 in	r=3.0 in
0.0	251.33	376.99	502.66	628.32	750.99
0.005	223.56	335.33	447.12	558.89	668.01
0.01	196.89	295.33	393.78	492.23	588.33
.02	150.04	225.06	300.09	375.11	448.34
.03	112.09	168.14	224.19	280.23	334.94
.04	82.74	124.11	165.48	206.84	247.23
.05	60.65	90.97	121.29	151.61	181.21
.06	44.23	66.35	88.47	110.58	132.17
.07	32.20	48.29	64.39	80.49	96.21
.08	23.32	34.98	46.65	58.31	69.69
.09	16.86	25.30	33.73	42.16	50.39
.10	12.16	18.25	24.33	30.41	36.35
.11	8.72	13.08	17.44	21.80	26.06
.12	6.21	9.31	12.42	15.52	18.55
.13	4.37	6.56	8.75	10.93	13.07
.14	3.04	4.56	6.08	7.60	9.09
.15	2.09	3.13	4.17	5.22	6.23
.16	1.38	2.07	2.76	3.46	4.13
.17	0.85	1.28	1.71	2.14	2.55
.18	0.48	0.72	0.96	1.19	1.43
.19	0.21	0.31	0.41	0.52	0.62
.20	0.05	0.08	0.10	0.13	0.15

TABLE A6. Dimensionless radial (F) and tangential (G) velocity components for mineral oil ( $\nu$  = .087 in  $^2/\text{sec.}$ ) flowing on a disk-rotating at both 1000 rpm and  $^2400$  rpm.

		N = 1000 rpm		:1	N = 2400 rpm	
z (in)	ς =34.69z	F (radia	ু (tangential)	5 7 4 Z	F (radia	G (tangential)
						)
0	0	0	00	0	0	00.
0.005	0.1734	920	892	26	104	0.8370
.01	.34	.124	.791	.537	.15	.688
0	.69	.173	609.	.07	.178	.455
0.	0.0	.179	.460	.61	.147	.284
0.	.38	.163	.344	.15	.107	.177
0.	.73	.138	.255	. 68	.073	.110
0	.08	.112	.188	.22	.048	.068
0.	. 42	.089	.139	.76	.031	.041
0.	.77	.069	.102	.29	.019	.025
0.	.12	.052	.074	.83	.012	.015
٦.	94.	.039	.054	.37	.007	.008
	.81	.029	.039	.91	.004	.004
٦.	.16	.022	.028	744	.002	.002
٦.	.51	.016	.020	.98	.001	.000
۲.	.85	.012	.014	.52	.001	.000
	.20	.008	.010	.06	.000	.001
٦.	.55	900.	.007	.598	.000	.001
٦.	5.89	.004	007	.13	.000	.001
.18	6.24	.003	.002	.67	.000	.001
۲.	.5	0.	00.	.2	0	00.
3	. 93	.001	000.	0.74	000.	.002

TABLE A7. Radial velocity components for mineral oil ( $\nu$  = .087 in<sup>2</sup>/sec.) flowing on a disk rotating at 1000 rpm.

z		Radial	Velocity	(ips) u=rωF	
(in)	r=1.0 in	r=1.5 in	r=2.0	in <b>r=2.5</b> in	r=3.0 in
0.0	0.00	0.0	0.0	0.0	0.0
0.005	8.01	12.01	16.02	20.02	24.03
0.01	13.07	19.60	26.14	32.67	39.20
0.02	18.18	27.27	36.36	45.45	54.54
0.03	18.76	28.15	37.53	46.91	56.30
0.04	17.07	25.60	34.14	42.67	51.21
0.05	14.49	21.74	28.97	36.23	43.48
0.06	11.79	17.69	23.58	29.48	35.37
0.07	9.32	13.98	18.64	23.30	27.96
0.08	7.25	10.87	14.49	18.12	21.74
0.09	5.49	8.23	10.97	13.72	16.46
0.10	4.14	6.20	8.27	10.34	12.41
0.11	3.10	4.65	6.20	7.75	9.30
0.12	2.30	3.46	4.61	5.76	6.91
0.13	1.71	2.57	3.42	4.28	5.13
0.14	1.26	1.89	2.53	3.16	3.79
0.15	•93	1.39	1.86	2.32	2.78
0.16	.68	1.02	1.36	1.70	2.04
0.17	.50	0.74	•99	1.24	1.49
0.18	.36	0.54	.72	.90	1.08
0.19	.26	0.39	.52	.65	.78
0.20	.18	0 28	.37	.46	•55

TABLE A8. Tangential velocity components for mineral oil ( $\nu$  = .087 in<sup>2</sup>/sec.) flowing on a disk rotating at 1000 rpm.

Z		Tangential	Velocity (in	os) V=rwG	
(in)	r=1.0 in	r=1.5 in	-	r=2.5 in	r=3.0 in
,,					J
0.0	104.72	157.08	209.44	261.80	314.16
0.005	93.41	140.11	186.82	233.53	280.23
0.01	82.93	124.39	165.86	207.32	248.78
0.02	63.82	95.72	127.63	159.54	191.45
0.03	48.23	72.35	96.47	120.59	144.70
0.04	36.06	54.08	72.11	90.14	108.17
0.05	26.76	40.13	53.51	66.89	80.27
0.06	19.77	29.66	39.54	49.43	59.31
0.07	14.57	21.85	29.13	36.42	43.70
0.08	10.69	16.04	21.38	26.73	32.08
0.09	7.83	11.75	15.67	19.58	23.50
0.10	5.71	8.56	11.41	14.27	17.12
0.11	4.16	6.24	8.31	10.39	12.47
0.12	3.01	4.51	6.01	7.51	9.02
0.13	2.16	3.24	4.32	5.40	6.48
0.14	1.54	2.30	3.07	3.84	4.61
0.15	1.07	1.61	2.15	2.69	3.22
0.16	.73	1.10	1.47	1.84	2.20
0.17	.48	.72	.97	1.21	1.45
0.18	.30	. 45	.60	.75	.90
0.19	.16	.24	.32	.40	.48
0.20	.06	.09	.12	.15	.18

TABLE A9. Radial velocity components for mineral oil ( $\nu$  = .087 in<sup>2</sup>/sec.) flowing on a disk rotating at 2400 rpm.

z		Radial	Velocity (ips	s) n=rwF	
(in)	r=1.0 in		r=2.0 in		r=3.0 in
0.0	0.0	0.0	0.0	0.0	0.0
0.005	26.34	39.51	52.68	65.85	78.70
0.01	39.84	59.75	79.67	99.59	119.03
0.02	44.79	67.18	89.57	111.97	133.83
0.03	37.07	55.61	74.14	92.68	110.77
0.04	27.04	40.56	54.09	67.61	80.81
0.05	18.47	27.71	36.96	46.18	55.20
0.06	12.14	18.21	24.28	30.35	36.27
0.07	7.79	11.69	15.58	19.48	23.28
0.08	4.93	7.39	9.85	12.32	14.72
0.09	3.08	4.63	6.17	7.71	9.25
0.10	1.91	2.87	3.82	4.78	5.72
0.11	1.18	1.76	2.35	2.94	3.51
0.12	.71	1.07	1.42	1.78	2.13
0.13	.42	.63	. 85	1.06	1.27
0.14	.24	.36	. 48	.61	.72
0.15	.13	.19	.26	.32	.39
0.16	.06	.09	.12	.15	.18
0.17	.02	.02	.03	.04	.05

TABLE Alo. Tangential velocity components for mineral oil ( $\nu$  = .087 in²/sec.) flowing on a disk rotating at 2400 rpm.

z			Velocity (in		
(in)	r=1.0 in	r=1.5 in	r=2.0 in	r=2.5 in	r=3.0 in
0.0	251.33	376.99	502.66	628.32	<b>7</b> 50 <b>.</b> 99
0.005	210.36	315.54	420.73	525.90	628.58
0.01	172.92	259.37	345.83	432.28	516.68
0.02	114.48	171.72	22 <b>8.</b> 96	286.20	342.08
0.03	71.43	107.14	142.86	178.57	213.43
0.04	44.69	67.03	89.37	111.72	133.53
0.05	2 <b>7.7</b> 5	41.62	55.49	69.37	82.91
0.06	17.14	25.71	34.28	42.85	51.22
0.07	10.48	15.72	20.96	26.20	31.32
0.08	6.36	9.54	12.72	15.90	19.00
0.09	3.76	5.64	7.52	9.40	11.23
0.10	2.15	3.22	4.29	5.37	6.41
0.11	1.14	1.71	2.28	2.85	3.40
0.12	.51	.77	1.03	1.28	1.53
0.13	.12	.17	.23	.29	• 35
0.14	13	19	26	32	38
0.15	28	42	56	70	84
0.16	38	- , , 56	- ,75	94	-1,12
0.17	44	65	87	-1.09	-1.30
0.18	47	71	95	-1.18	-1,41

#### APPENDIX B

#### Streamlines in the $r-\theta$ Plane

TABLE B1. Determination of streamlines in r-0 plane for 10.2 gpm flow of hydraulic oil ( $\nu$  = .194) onto a disk rotating at 1000 rpm.

Test No. 1 Q = 10.2 gpm  $\nu$  = .194 in<sup>2</sup>/sec. N = 1000 rpm (a) Surface Streamline

 $\theta_{S} = 1.146 \text{ r} - .808 \text{ ln r} - 1.587$ 

Radius r (in)	Depth h (in)	u <sub>s</sub> (ips)	v <sub>s</sub> (ips)	$v_{\mathrm{s}}/\mathrm{u}_{\mathrm{s}}$	(degrees)
1.80	.200	2.74	3.41	1.25	0
2.00	.112	16.4	25.0	1.53	8.3
2.25	.082	29.6	52.0	1.76	19.3
2.50	.066	40.1	80.0	2.00	30.8
2.75	.056	44.9	107.1	2.38	42.8
3.00	.048	51.9	136.3	2.63	55.1

# (b) Average Streamline $\theta_{\Lambda} = 1.776 \text{ r} - .209 \text{ ln r} - 3.073$

Radius r (in)	Depth h (in)	u <sub>A</sub> (ips)	v <sub>A</sub> (1ps)	v <sub>A</sub> /u <sub>A</sub>	θ <sub>A</sub> (degrees)
1.80	.200	17.3	52.2	3.02	0
2.00	.112	27.8	93.3	3.36	13.4
2.25	.082	33.8	127.5	3.77	43.1
2.50	.066	37.8	158.3	4.18	67.3
2.75	.056	40.5	186.5	4.60	91.7
3.00	.048	41.8	218.0	5.21	116.1

TABLE B2. Determination of streamlines in  $r-\theta$  plane for 10.2 gpm flow of hydraulic oil ( $\nu$  = .194) onto a disk rotating at 2400 rpm

Test No. 2 Q = 10.2 gpm  $v = .194 \text{ in}^2/\text{sec}$ . N = 2400 rpm (a) Surface Streamline

$$\theta_s = 1.226 \text{ r} - .479 \text{ ln. r} - 1.582$$

Radius r (in)	Depth h (in)	u <sub>s</sub> (ips)	v <sub>s</sub> (ips)	v <sub>3</sub> /u <sub>s</sub>	θέ (degrees)
1.43	.200	. 49	.07		0
1.50	.100	13.4	18.03	1.36	3.6
1.75	.059	48.2	80.0	1.66	12.9
2.00	.042	77.6	156.6	2.02	30.8
2.25	.036	100.3	222.4	2.22	45.2
2.50	.029	111.7	289.7	2.60	59.8
2.75	.026	122.0	349.4	2.86	75.0
3.00	.022	132.0	425.6	3.23	89.7

# (b) Average Streamline $\theta_{\Delta} = 2.030 - .042 \ln r - 2.888$

Radius r (in)	Depth h (in)	uA (ips)	VA (ips)	v <sub>A</sub> /u <sub>A</sub>	θA (degrees)
1.43	.200	21.8	62.5	2.87	0
1.50	.100	41.6	125.0	3.00	8.0
1.75	.059	60.3	212.0	3.52	31.0
2.00	.042	74.2	298.0	4.02	65.5
2.25	.036	78.0	352.0	4.51	94.2
2.50	.029	86.0	431.0	5.02	123.2
2.75	.026	87.3	481.0	5.52	151.8
3.00	.022	93.3	568.0	6.08	180.6

TABLE B3. Determination of streamlines in  $r-\theta$  plane for 5.0 gpm flow of hydraulic oil ( $\nu$  = .194) onto a disk rotating at 1000 rpm.

Test No. 3 Q = 5.0 gpm  $v = .194 \text{ in}^2/\text{sec.}$  N = 1000 rpm (a) Surface Streamline  $\theta_S = 1.302 \text{ r} - .315 \text{ ln r} - 1.557$ 

Radius r (in)	Depth h (in)	u <sub>s</sub> (ips)	v <sub>s</sub> (ips)	v <sub>s</sub> /u <sub>s</sub>	θ <sub>S</sub> (degrees)
1.25	.240	.6	.7	1.17	0
1.50	.093	16.8	27.8	1.66	15.4
1.75	.067	28.0	54.9	1.96	31.2
2.00	.053	35.9	82.0	2.28	47.5
2.25	.045	42.0	109.6	2.61	64.0
2.50	.038	46.9	137.6	2.93	80.8
2.75	.033	50.6	165.1	3.26	97.7
3.00	.029	53.8	194.7	3.61	114.8

### (b) Average Streamline $\theta_{\Lambda} = 2.352 \text{ r} + .116 \text{ ln r} - 2.966$

Radius r (in)	Depth h (in)	u <sub>A</sub> (ips)	VA (ips)	v <sub>A</sub> /u <sub>A</sub>	θ <sub>A</sub> (degrees)
1.25	.240	10.2	30.6	3.00	0
1.50	.093	21.0	79.0	3.75	34.9
1.75	.067	26.1	109.8	4.20	69.6
2.00	.053	28.9	138.6	4.79	104.1
2.25	.045	30.6	.165.2	5.40	138.6
2.50	.038	32.3	193.5	5.99	173.0
2.75	.033	33.3	219.5	6.59	207.3
3.00	.029	35.3	253.5	7.18	241.6

TABLE B4. Determination of streamlines in  $r-\theta$  plane for 5.0 gpm flow of hydraulic oil ( $\nu$  = .194) onto a disk rotating at 2400 rpm.

Test No. 4 Q = 5.0 gpm  $v = .194 \text{ in}^2/\text{sec}$ . N=2400 rpm (a) Surface Streamline  $\theta_S = 1.725 \text{ r} - .447 \text{ ln r} - 1.725$ 

Radius r (in)	Depth h (in)	u <sub>s</sub> (ips)	v <sub>s</sub> (ips)	v <sub>s</sub> /u <sub>s</sub>	θs (degrees)
1.000	.210	.23	.14		0
1.25	.055	37.3	64.5	1.76	19.2
1.50	.038	61.6	132.9	2.16	39.0
1.75	.030	78.7	199.3	2.53	59.8
2.00	.024	88.7	269.7	3.04	81.1
2.25	.021	98.7	329.0	3.34	102.7
2.50	.018	104.2	398.5	3.82	124.9
2.75	.016	108.0	463.1	4.28	147.1
3.00	.014	110.4	532.3	4.82	169.6

# (b) Average Streamline $\theta_A = 2.977 \text{ r} - 2.977$

Radius r (in)	Depth h (in)	uA (ips)	VA (ips)	v <sub>A</sub> /u <sub>A</sub>	θA (degrees)
1.00	.210	14.6	43.3	2.97	0
1.25	.055	44.5	165.5	3.72	37.9
1.50	.038	53.8	240.0	4.46	85.2
1.75	.030	59.3	309.0	5.21	127.8
2.00	.024	63.8	379.5	5.95	170.6
2.25	.021	64.9	433.0	6.68	213.2
2.50	.018	67.1	506.0	7.53	255.8
2.75	.016	69.7	569.0	8.16	298.5
3.00	.014	73.0	650.0	8.90	341.1

TABLE B5. Determination of streamlines in r-0 plane for 10.2 gpm flow of mineral oil ( $\nu$  = .087) onto a disk rotating at 1000 rpm.

Test No. 5 Q = 10.2 gpm  $v = .087 \text{ in}^2/\text{sec.}$  N = 1000 rpm (a) Surface Streamline  $\theta_S = .940 \text{ r} - .764 \text{ ln r} - 1.454$ 

Radius r (in)	Depth h (in)	u <sub>s</sub> (ips)	v <sub>s</sub> (ips)	v <sub>s</sub> /u <sub>s</sub>	θs (degrees)
2.18	.200	. 4	.13		0
2.25	.111	6.7	9.1	1.36	2.3
2.50	.072	22.2	34.5	1.55	11.2
2.75	.055	36.1	64.0	1.77	20.6
3.00	.044	48.1	101.0	2.10	30.1

### (b) Average Streamline $\theta_A = 1.454 \text{ r} - .305 \text{ ln r} - 2.932$

Radius r (in)	Depth h (in)	u <sub>A</sub> (ips)	VA (ips)	v <sub>A</sub> /u <sub>A</sub>	θA (degrees)
2.18	.200	14.3	41.2	2.88	0
2.25	.111	25.0	74.3	2.98	5.3
2.50	.072	34.6	114.6	3.31	24.3
2.75	.055	41.3	150.0	3.64	43.5
3.00	.044	45.7	187.6	4.10	62.9

TABLE B6. Determination of streamlines in  $r-\theta$  plane for 10.2 gpm flow of mineral oil ( $\nu = .087$ ) onto a disk rotating at 2400 rpm.

Test No. 6 Q = 10.2 gpm  $v = .087 \text{ in}^2/\text{sec.}$  N = 2400 rpm (a) Surface Streamline

 $\theta_s = .728 r + .266 ln r - 1.423$ 

Radius	Depth	u <sub>s</sub>	vs	v <sub>s</sub> /u <sub>s</sub>	θ <sub>s</sub>
r (in)	h (in)	(ips)	(ips)		(degre <b>e</b> s)
1.75	.180	02	83		0
2.00	.047	42.1	75.7	1.80	12.4
2.25	.034	74.7	136.6	1.84	24.7
2.50	.028	96.6	200.1	2.07	36.7
2.75 3.00	.023	116.2	275.7 336.5	2.18	48.6 60.3

### (b) Average Streamline $\theta_{\Delta} = 1.686 \text{ r} - .002 \text{ ln r} - 2.949$

Radius r (in)	Depth h (in)	u <sub>A</sub> (ips)	VA (ips)	v <sub>A</sub> /u <sub>A</sub>	θ <sub>A</sub> (degrees)
1.75	.180	19.8	58.3	2.94	0
2.00	.047	66.3	223.5	3.37	22.2
2.25	.034	81.5	309.0	3.80	48.2
2.50	.028	89.0	375.0	4.22	72.4
2.75	.023	98.7	457.0	4.63	96.5
3.00	.020	101.3	512.0	5.05	120.7

TABLE B7. Determination of streamlines in r-0 plane for 5.0 gpm flow of mineral oil ( $\nu$  = .087) onto a disk rotating at 1000 gpm.

Test No. 7 Q = 5.0 gpm  $\nu$  = .087 in  $^2/\text{sec}$ . N = 1000 rpm (a) Surface Streamline

$$\theta_{S} = 1.114 \text{ r} - .418 \text{ ln r} - 1.535$$

Radius r (in)	Depth h (in)	u <sub>s</sub> (ips)	v <sub>s</sub> (ips)	v <sub>s</sub> /u <sub>s</sub>	θ <sub>S</sub> (degrees)
1.54	.200	.29	.09		0
1 <b>.7</b> 5	.076	14.1	21.4	1.52	10.3
2.00	.052	27.9	50 <b>.7</b>	1.82	23.1
2.25	.041	37.8	79.0	2.09	36.2
2.50	.034	45.2	108.4	2.40	49.7
2.75	.030	51.1	132.6	2.60	63.4
3.00	.026	55.6	163.4	2.94	77.2

#### (b) Average Streamline

 $\theta_{A} = 1.919 \text{ r} - .0135 \text{ ln r} - 2.949$ 

Radius r (in)	Depth h (in)	u <sub>A</sub> (ips)	v <sub>A</sub> (ips)	v <sub>A</sub> /u <sub>A</sub>	θ <sub>A</sub> (degrees)
1.54	.200	9.95	29.5	2.97	0
1.75	.076	23.1	77.6	3.37	23.0
2.00	.052	29.5	113.4	3.85	50.4
2.25	.041	33.3	144.0	4.33	77.8
2.50	.034	36.0	173.5	4.81	105.2
2.75	.030	37.2	196.7	5.29	132.6
3.00	.026	39.3	227.0	5.77	160.0

TABLE B8. Determination of streamlines in r-0 plane for 5.0 gpm flow of mineral oil ( $\nu$  = .087) onto a disk rotating at 2400 rpm.

Test No. 8 Q = 5.0 gpm  $v = .087 \text{ in}^2/\text{sec.}$  N = 2400 rpm (a) Surface Streamline  $\theta_S = 1.523 \text{ r} - .613 \text{ ln r} - 1.758$ 

Radius r (in)	Depth h (in)	u <sub>s</sub> (ips)	v <sub>s</sub> (ips)	v <sub>s</sub> /u <sub>s</sub>	θs (degrees)
1.23	.180	02	58		0
1.25	.093	3.42	4.10	1.20	•5
1.50	.038	43.6	75.0	1.73	16.7
1.75	.028	67.6	140.1	2.07	32.3
2.00	.022	86.5	211.8	2.45	50.5
2.25	.0185	99.1	277.3	2.80	67.2
2.50	.016	107.0	354.6	3.31	85.3
2.75	.014	114.7	410.3	3.58	103.8
3.00	.0125	122.7	473.1	3.86	122.5

# (b) Average Streamline $\theta_A = 2.536 \text{ r} - .316 \text{ ln r} - 3.054$

Radius r(in)	Depth h (in)	u <sub>A</sub> (ips)	v <sub>A</sub> (ips)	v <sub>A</sub> /u <sub>A</sub>	θ <sub>A</sub> (degrees)
1.23	.180	13.9	42.2	3.05	0
1.25	.093	26.9	81.7	3.04	2.6
1.50	.038	62.5	200.0	3.20	35.6
1.75	.028	68.7	271.5	3.95	69.2
2.00	.022	73.7	345.4	4.68	103.1
2.25	.0185	76.7	411.0	5.36	137.3
2.50	.016	79.6	475.0	5.97	171.7
2.75	.014	79.6	543.0	6.71	206.3
3.00	.0125	81.8	608.0	7.43	241.1

